A Parametric Study of Gross Building Coverage Ratio (GBCR) Variation on Outdoor Ventilation in Singapore's High-rise Residential Estates

Rou-Xuan Lee[*1], Nyuk-Hien Wong[2]

[*1,2]Department of Building, School of Design and Environment, National University of Singapore
4 Architecture Drive, Singapore 117566, Singapore

[*1]g0800515@nus.edu.sg; [2]bdgwnh@nus.edu.sg

***Abstract*-Gross Building Coverage Ratio (GBCR) is one of the urban morphological variables that have an effect on microclimate within the urban canopy level (UCL). It is usually defined as the ratio between gross ground floor area covered by all buildings to a given site area. The impact of different morphological scenarios for GBCR variation on external ventilation levels within a typical high-rise Housing and Development Board (HDB) residential estate (or precinct) in Singapore is analyzed through a parametric study exercise. This is done by utilizing three-dimensional numerical simulations with the Reynolds-averaged Navier-Stokes (RANS) Realizable k-ε turbulence model (RLZ) from the commercial computational fluid dynamics (CFD) code Star-CCM+. Wind tunnel tests were carried out in order to validate the simulation software's accuracy before put in use for the parametric study. Both the study results agree reasonably well here. External ventilation levels are quantified using the area-averaged Wind Velocity Ratio (V_R) index, an indication of the average outdoor ventilation potential within an estate at a certain level. Two types of common HDB block types in Singapore are examined – point and slab blocks in three types of configurations: (i) random, (ii) group and (iii) courtyard. Measurements are taken at both the pedestrian and mid-levels under different wind orientations. From the study results, consistent trends can be observed as using the same GBCR value produces different results of average outdoor wind speed within an estate or precinct, under different block types, wind orientations and configurations.**

Keywords- Gross Building Coverage Ratio (GBCR); Morphological Variables; Wind Velocity Ratio (V_R); Outdoor Ventilation; High-Rise Residential Estate; Parametric Study; Computational Fluid Dynamics (CFD)

I. INTRODUCTION

The urbanization trend that comes with the surge of urban population has caused a host of environmental problems such as higher air temperatures, high pollution levels and lower wind flow rates. Unstructured and improper planning of urban morphologies has become prevalent in rapid urbanization areas and, in particularly, wind speed is being seriously decreased due to the buildings' roughness and geometry within [1]. The climate of urban canyons is primarily controlled by micrometeorological effects of canyon geometry, rather than the mesoscale forces controlling urban boundary layer (UBL) climatic systems [2]. One good way to counteract or reduce outdoor ventilation problems is to go for designs that are optimized for ample outdoor ventilation, so as to dissipate built-up heat within through the process of turbulent transfer. Numerous studies made in previous field experiments, wind tunnel simulations and computational fluid dynamics (CFD) modeling have shown us that different near-surface wind flow regimes can result from the way urban canyons are structured.

Based on the literature review, the seven morphological variables that determine and have an association with natural outdoor ventilation within a high-rise residential precinct are Orientation [3-5], Building Shape [6], Gross Building Coverage Ratio [5, 7-12], Geometry [11, 13-15], Permeability [3, 7], Buildings' Height Variation [5, 16, 17] and Staggering of Blocks Arrangement [5, 12, 18, 19]. These studies by previous researchers postulate that there is an association between the different morphological variables and outdoor ventilation potential. This paper will focus on a detailed parametric study on the effects of one of them – Gross Building Coverage Ratio (GBCR) on external ventilation levels within a typical high-rise Housing and Development Board (HDB) public residential estate (or precinct) here in Singapore.

The term GBCR can be explained as the ratio between gross ground floor area covered by all buildings to a given site area. In an urban environment, the presence of numerous obstacles significantly increases the ground roughness and thermal mass of urban fabric as compared to a rural environment. Therefore, friction effect on airflow increases, causing a reduction in average outdoor wind speed and increased turbulence intensity when wind moves from countryside to an urban environment. Golany defined GBCR as a ratio between gross ground floor area of a building to a given site area $\lambda_p = \frac{\sum builtarea}{\sum builtarea + \sum unbuiltarea}$. It regulates development and describes what proportion of land area would be utilized for development [9]. Zhang et al. defined the same concept with a term called 'plan area density' $\lambda_{area} = \left(\sum_{i=1}^{n} B_i L_i\right) / A_{total}$, where n is the number of buildings; B_i and L_i is the building width and length, respectively, and A_{total} is the total plan area [12]. Kubota et al. carried out a wind tunnel test of 22 residential Japanese neighborhoods (actual urban field cases) and concluded that there is a strong relationship between GBCR (building density) and the mean wind velocity ratio at pedestrian level in residential neighborhoods, without

considering the other morphological variables [10]. Ng further supported Kubota's existing findings when he concluded that building site coverage impacts more than building height on pedestrian wind environment [5]. Givoni, Brown and Dekay findings point to an increase in building density will reduce the wind velocity in the urban area, due to the increased friction near the ground [7, 8]. Oke's findings also show a general trend that an increase in GBCR decreases the mean wind velocity at the pedestrian level for a given aspect ratio of canyons. However, in the case for urban boundary layer (UBL), such influence occurs with increasing building density up to a peak and then declines above the urban canopy layer (UCL) due to the interference between the individual wakes that smother their turbulence production roles [11]. UBL wind, which is situated above the UCL, is highly related to the roughness length of a ground surface and has some influence upon the UCL winds particularly at the upper levels. Hence, if the aspect ratios for the canyons are very high, it will have lesser influence of the pedestrian winds.

A comprehensive parametric numerical study has been carried out to explore the association of GBCR with the area-averaged **Wind Velocity Ratio (V_R)** index, an indication of the average outdoor ventilation potential within an estate at a certain level. This was done using three-dimensional numerical simulations with the Reynolds-averaged Navier-Stokes (RANS) Realizable k-ε turbulence model (RLZ) by the commercial computational fluid dynamics (CFD) code Star-CCM+, to study the impact of different morphological scenarios of GBCR variation. Such systematic studies are far difficult to be realized in real streets and relatively costly in wind tunnels; hence, CFD simulations offer an appealing alternative in this occasion. Two types of common HDB block types in Singapore were examined – point and slab blocks, in three types of GBCR configurations: (i) random, (ii) group and (iii) courtyard variation at both the pedestrian and mid-levels under different wind orientations. This CFD software, Star-CCM+, is not commonly applied in atmospheric wind studies, hence a wind tunnel test was carried out in order to validate its accuracy before made into use for the parametric study. The numerical results agreed reasonable well with the commissioned wind tunnel results.

The objective of the present work is to investigate how the magnitude of outdoor ventilation within a precinct, vary with the GBCR values. The detailed methodology adopted and the results obtained will be discussed in the following sections. We can see that from the study results, consistent trends can be observed as using the same GBCR value produces different results of area-averaged V_R within a precinct under different block types, wind orientation and configurations. But in prior to this conclusion, the design principles of HDB blocks and their site planning will be briefly discussed at the beginning part of this paper to facilitates readers' idea of how Singapore's public high-rise residential estates were developed.

II. BUILDING DESIGNS AND SITE PLANNING

The design principles and precinct planning of HDB flats and their estates are important as they affect the development. There are mainly two common physical forms of block designs – point block and slab block. Most slab blocks are about 10 to 14 storey high (of 3, 4 or 5-room units mix), and each floor is served by a single corridor and lift/s (Fig. 1a). Point blocks are about 20 to 25 storey high and have a central core with lift/s and staircase that serves 4 units (mostly 5-room flats) in each floor (Fig. 1b). The latter are often arranged in clusters of twos or threes to be identified as site landmarks in an estate. Generally, the block design is very much affected by the flat unit type and mix, site and town planning consideration, number of units per block, height restriction within that area, population, demographics, etc. Fig. 2 shows an overall concept plan of Singapore showing the different types of land use, with about 50% of the land for residential use [20] (Fig. 2).

For the site and town planning consideration, four main factors are observed [21]:

1. Residential density determination - calculated by the number of dwelling units on a site over the net site area (including car parks, commercial areas, etc.). It is measured in terms of dwelling units per hectare (du/h).
2. Spacing of building blocks - largely determined by height of the buildings blocks, its influencing factors include car-parking requirements, open spaces, cost, construction technology, lift-ratio and proportionate scale. The latest Public Housing Design Guide [22], stipulates the spacing between buildings should be generally determined qualitatively based on:
   - Storey height of buildings – a wider spacing is required between taller buildings.
   - Overlap distance of the buildings – a wider spacing is required for buildings with larger overlap.
   - Building relationship, in terms of (1) front/rear to front/rear; (2) front/rear to side; (3) side to side; (4) front/rear to multi-storey car park; (5) side to multi-storey car park. Wider spacing is provided for facades with openings. Facades with openings are considered the front or rear of buildings and facades with no openings are the sides of the buildings.
3. The number of car-parking space and forms of car-parking. The demand for it is directly proportional to car ownership numbers, which is dependent on the level of society affluence, and also government measures to curb car population growth. Car parks come mainly in two forms – surface car parks (on the ground) and multi-storey car parks.
4. Environmental design. The primary issue is solar orientation where most slab blocks were orientated with their short sides facing east-west as much as possible.

(a)  (b) 

Fig. 1 (a) Slab and (b) point HDB blocks

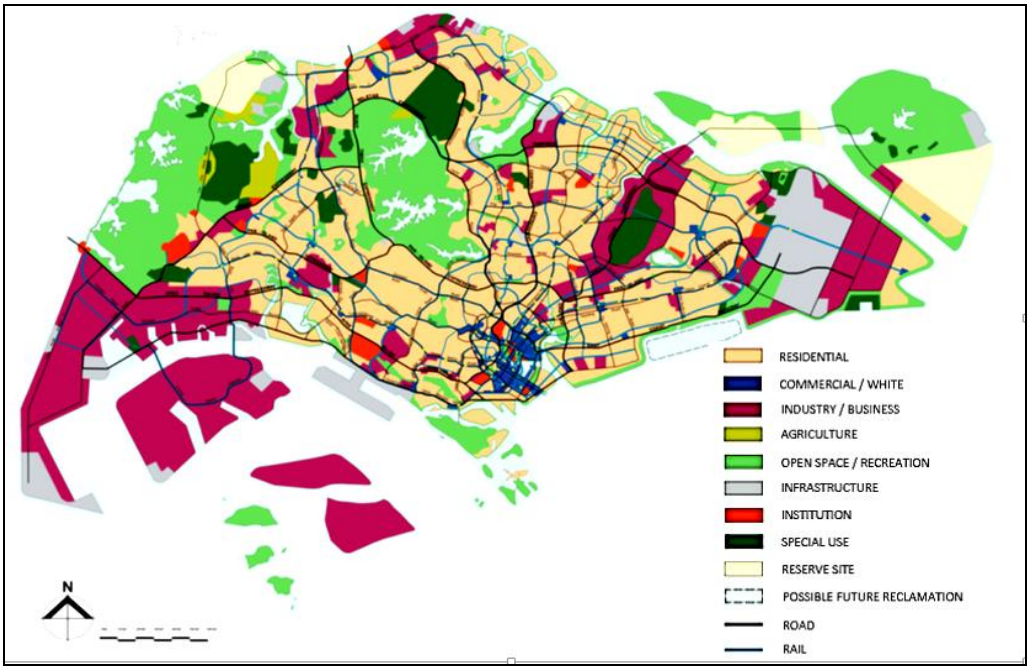

Fig. 2 Singapore Concept Plan (Latest revision at 2001, to be reviewed every 10 years) [20]

In 1980, HDB adopted a standard measure of 200du/h for its net residential density. This net figure has been increased throughout the years to take into account of the rising Singapore population through native birth rates and immigration. In relation to point 2, the increased demand for larger flats also meant that there are two options in block designs. One is to either reduce the building spacing and next is to increase the buildings height (subject to height restriction at the said area). The former is given priority preference before the latter because Singapore has the highest density of airports in the world (civilian and military) which impose height restrictions on buildings across most of the island as tall buildings are not possible near the flight paths of aircraft [23] (Fig. 3). Furthermore, buildings that are overly tall might block telecommunications microwave path or the line of sight of necessary satellite stations. However, there are attempts in some estates in central Singapore to build 30-to-40-storey blocks (higher than the usual 25-storey blocks) and in most estates where there are no height restrictions. But unfortunately, most areas in Singapore fall under the aviation zones. Next for point 3, more multi-storey car parks will be built to ease parking space demand and saving more space as the car ownership grows. Finally for point 4, due to land area scarcity, buildings orientation issues are overcome by effective use of open spaces, corresponding of building elevations on both sides of the street, variation of block heights with more low-rise blocks fronting the higher blocks, planting of more greenery like trees, using more cool materials and coatings on building facades, etc.

In Singapore, the sun is almost directly overhead throughout the year since it is located only 1 °north of the equator. East and west orientations receive the most solar exposure here and therefore have the most potential for solar heat gains (Fig. 4). Furthermore, wind directions here are predominantly N-NNE and S-SSE throughout the year (depending on the monsoon season) [24] (Fig. 5). It pays to have the longer sides of the building facing north and south for both solar and ventilation considerations.

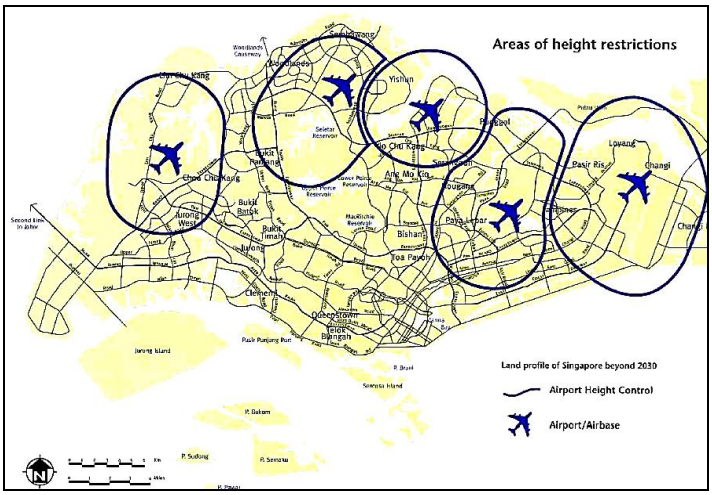

Fig. 3 Areas of height restriction in Singapore [23]

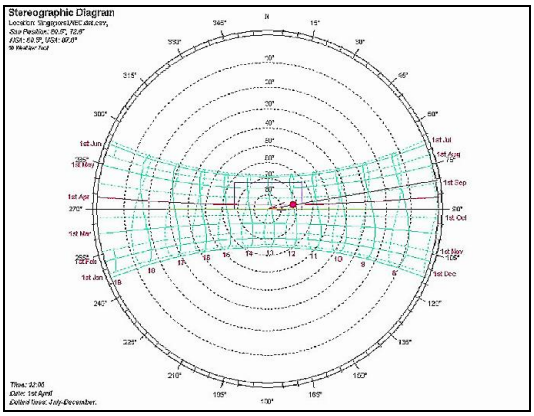

Fig. 4 Sun path diagram for Singapore (Left)

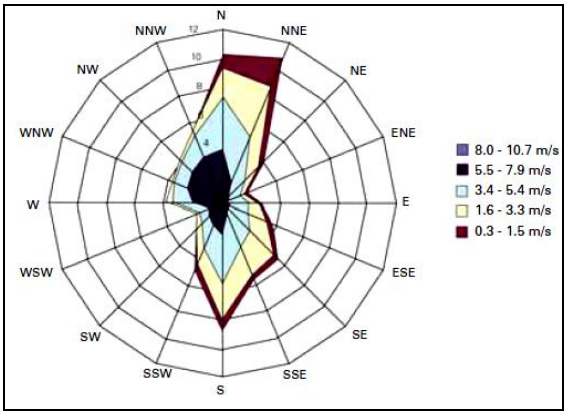

Fig. 5 Singapore wind rose data from Meteorological Service Singapore – Changi Station (1975 – 2006) [24] (Right)

III. METHODOLOGY

In this paper, an in-depth parametric study approach is adopted for the investigation of GBCR on average outdoor ventilation within a said precinct, and a numerical study is employed to simulate the conditions of a typical public HDB high-rise residential housing estate, which is set to a typical estate (precinct) size of approximately 500m×500m as the base case standard. The area-averaged outdoor velocity magnitude values will be extracted at the pedestrian level (cut at a constrained horizontal plane at 2m above ground, within the precinct) and mid-level (mid horizontal level of the average height of all buildings within the precinct) (Fig. 6). The mid-levels will be fixed at 56m and 25m above ground for point and slab blocks respectively. These mid-levels are based on the base cases of the respective block types and will be used throughout for extracting the outdoor average velocities. Outdoor velocity magnitude readings from all the cells within the highlighted box for the studied level are area-averaged (according to cell size) over the total area of all cells at the same level.

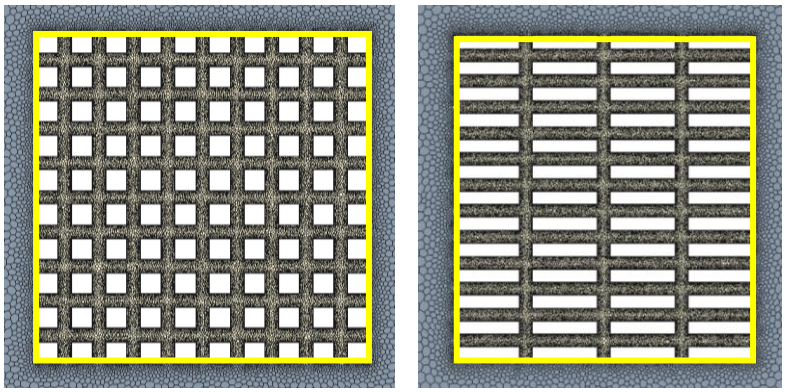

Fig. 6 Point (L) and slab (R) blocks layout in a 500×500m HDB estate

A. GBCR Values and Configuration Types

For comparison, two base case scenarios are used here, one for the **point blocks** (each block dimension is 30L×30W×112H metres) and another for **slab blocks** (each block dimension is 100L×20W×50H metres) whereby both are the most commonly adopted building shapes in Singapore. The base case spacing between the blocks is 20m apart. All the blocks are confined within a 500×500m HDB estate, assumed to be the existing maximum size for high density living in Singapore, given the current regulations and control.

The three different types of GBCR configuration types that will be studied here for both types of point and slab blocks for their effects in area-averaged V_R at the pedestrian and mid-levels – random, group and courtyard (Figs. 7, 8, 9, 10, 11 and 12).

- Random GBCR variation refers to the buildings, under different GBCR values, will be randomly spread evenly around within the precinct. The spacing between the buildings will be as similar as possible to ensure an even distribution.
- Group GBCR variation refers to the buildings that are grouped into a cluster together with no spreading around the precinct at all.
- Courtyard GBCR refers to empty spaces within a precinct that are designed as courtyards or patches of spaces where people can use for different activities.

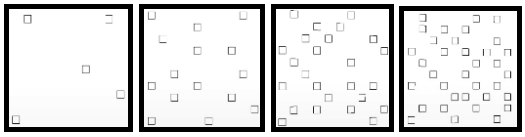

(a) 0.018 (b) 0.054 (c) 0.090 (d) 0.126

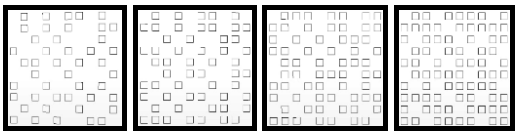

(e) 0.162 (f) 0.198 (g) 0.234 (h) 0.270

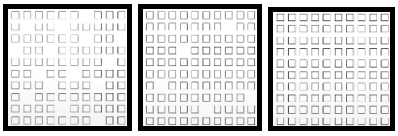

(i) 0.306 (j) 0.342 (k) 0.360

Fig. 7 GBCR ratio for point blocks random configuration

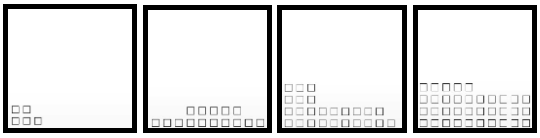

(a) 0.018 (b) 0.054 (c) 0.090 (d) 0.126

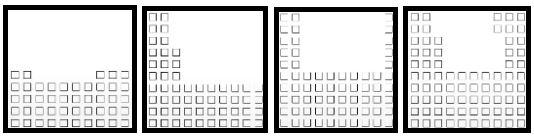

(e) 0.162 (f) 0.198 (g) 0.234 (h) 0.270

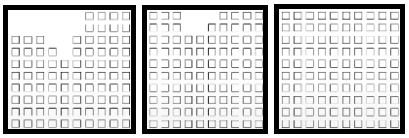

(i) 0.306 (j) 0.342 (k) 0.360

Fig. 8 GBCR ratio for point blocks group configuration

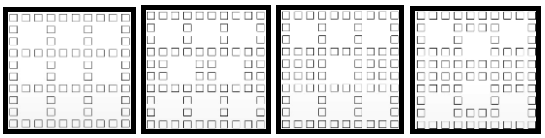

(a) 0.230 (b) 0.245 (c) 0.259 (d) 0.274

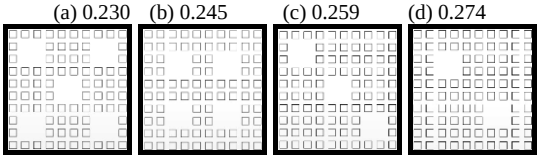

(e) 0.288 (f) 0.302 (g) 0.317 (h) 0.331

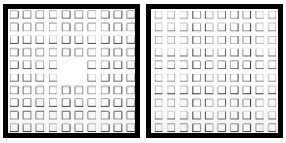

(i) 0.346 (j) 0.360

Fig. 9 GBCR ratio for point blocks courtyard configuration

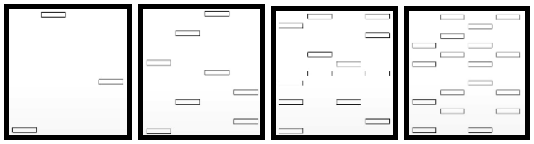

(a) 0.024 (b) 0.064 (c) 0.104 (d) 0.144

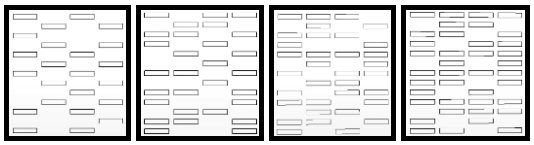

(e) 0.184 (f) 0.232 (g) 0.272 (h) 0.312

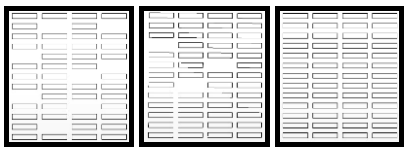

(i) 0.352 (j) 0.392 (k) 0.416

Fig. 10 GBCR ratio for slab blocks random configuration

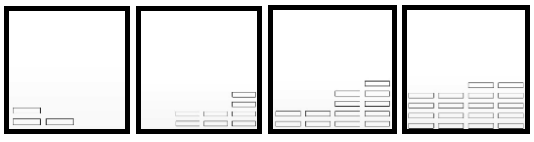

(a) 0.024 (b) 0.064 (c) 0.104 (d) 0.144

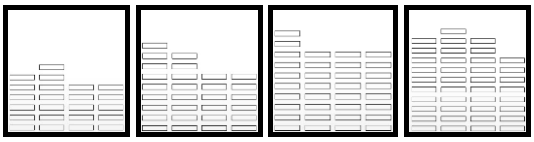

(e) 0.184 (f) 0.232 (g) 0.272 (h) 0.312

(i) 0.352 (j) 0.392 (k) 0.416

Fig. 11 GBCR ratio for slab blocks group configuration

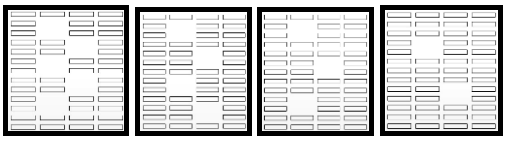

(a) 0.336 (b) 0.352 (c) 0.368 (d) 0.384

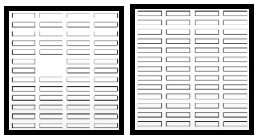

(e) 0.400 (f) 0.416

Fig. 12 GBCR ratio for slab blocks courtyard configuration

The morphological index that is used to quantify GBCR in this study will follow Golany's format namely, $\lambda_p = \frac{\sum builtarea}{\sum builtarea + \sum unbuiltarea}$ [9]. The GBCR values used in this parametric study are as shown in Tables 1 and 2 for both the point and slab blocks study respectively.

TABLE 1 TABULATED VALUES OF GBCR FOR THE PARAMETRIC STUDY FOR RANDOM AND GROUP CONFIGURATIONS

POINT BLOCKS (Random & Group Configurations)			
Case	Description	% of Bldgs	GBCR
1	Point Blocks - GBCR - 5 out of 100 point blocks	5%	0.018
2	Point Blocks - GBCR - 15 out of 100 point blocks	15%	0.054
3	Point Blocks - GBCR - 25 out of 100 point blocks	25%	0.090
4	Point Blocks - GBCR - 35 out of 100 point blocks	35%	0.126
5	Point Blocks - GBCR - 45 out of 100 point blocks	45%	0.162
6	Point Blocks - GBCR - 55 out of 100 point blocks	55%	0.198
7	Point Blocks - GBCR - 65 out of 100 point blocks	65%	0.234
8	Point Blocks - GBCR - 75 out of 100 point blocks	75%	0.270
9	Point Blocks - GBCR - 85 out of 100 point blocks	85%	0.306
10	Point Blocks - GBCR - 95 out of 100 point blocks	95%	0.342
11	Point Blocks - BASE (TOTAL 100 blocks)	100%	0.360

SLAB BLOCKS (Random & Group Configurations)			
Case	Description	% of Bldgs	GBCR
1	Slab Blocks - GBCR - 3 out of 52 slab blocks	5%	0.024
2	Slab Blocks - GBCR - 8 out of 52 slab blocks	15%	0.064
3	Slab Blocks - GBCR - 13 out of 52 slab blocks	25%	0.104
4	Slab Blocks - GBCR - 18 out of 52 slab blocks	35%	0.144
5	Slab Blocks - GBCR - 23 out of 52 slab blocks	45%	0.184
6	Slab Blocks - GBCR - 29 out of 52 slab blocks	55%	0.232
7	Slab Blocks - GBCR - 34 out of 52 slab blocks	65%	0.272
8	Slab Blocks - GBCR - 39 out of 52 slab blocks	75%	0.312
9	Slab Blocks - GBCR - 44 out of 52 slab blocks	85%	0.352
10	Slab Blocks - GBCR - 49 out of 52 slab blocks	95%	0.392
11	Slab Blocks - BASE (TOTAL 52 blocks)	100%	0.416

TABLE 2 TABULATED VALUES OF GBCR FOR THE PARAMETRIC STUDY FOR COURTYARD CONFIGURATIONS

POINT BLOCKS (Courtyard Configuration)			
Case	Description	% of Bldgs	GBCR
1	Point Blocks - GBCR - 64 out of 100 point blocks	64%	0.230
2	Point Blocks - GBCR - 68 out of 100 point blocks	68%	0.245
3	Point Blocks - GBCR - 72 out of 100 point blocks	72%	0.259
4	Point Blocks - GBCR - 76 out of 100 point blocks	76%	0.274
5	Point Blocks - GBCR - 80 out of 100 point blocks	80%	0.288
6	Point Blocks - GBCR - 84 out of 100 point blocks	84%	0.302
7	Point Blocks - GBCR - 88 out of 100 point blocks	88%	0.317
8	Point Blocks - GBCR - 92 out of 100 point blocks	92%	0.331
9	Point Blocks - GBCR - 96 out of 100 point blocks	96%	0.346
10	Point Blocks - BASE (TOTAL 100 blocks)	100%	0.360

SLAB BLOCKS (Courtyard Configurations)			
Case	Description	% of Bldgs	GBCR
1	Slab Blocks - GBCR - 42 out of 52 slab blocks	80%	0.336
2	Slab Blocks - GBCR - 44 out of 52 slab blocks	84%	0.352
3	Slab Blocks - GBCR - 46 out of 52 slab blocks	88%	0.368
4	Slab Blocks - GBCR - 48 out of 52 slab blocks	92%	0.384
5	Slab Blocks - GBCR - 50 out of 52 slab blocks	96%	0.400
6	Slab Blocks - BASE (TOTAL 52 blocks)	100%	0.416

B. Numerical Simulations

In our research here, one of the RANS model variants - Realizable *k-ε* turbulence model (RLZ) is selected for use in the simulation studies. This is a revised *k-ε* turbulence model proposed by Shih et al. [25]. Solutions to the problem here utilized this turbulence model, in which the Navier-Stokes equations are discretized using a finite volume method and the SIMPLE algorithm is used to handle pressure-velocity coupling. The following set of discretized algebraic equations is solved by the segregated method.

The four types of partial differential equations that need to be solved are [25, 26]:

(1) Continuity equation

$$\frac{\partial u_j}{\partial x_j} = 0$$

(2) RANS equations (in x, y and z directions)

$$\frac{\partial u_i}{\partial t} + u_j \frac{\partial u_i}{\partial x_j} = -\frac{1}{\rho}\frac{\partial P}{\partial x_i} + \frac{\mu}{\rho}\frac{\partial^2 u_i}{\partial x_j \partial x_j} - \frac{\partial}{\partial x_j}(\overline{u_i' u_j'}) + g_i$$

(3) Turbulent kinetic energy (k) (m2s-2)

$$\frac{\partial k}{\partial t} + u_j \frac{\partial k}{\partial x_j} = \frac{1}{\rho}\frac{\partial}{\partial x_j}\left[\left(\mu + \frac{\mu_t}{\sigma_k}\right)\frac{\partial k}{\partial x_j}\right] + \frac{G_k}{\rho} - \varepsilon$$

(4) Dissipation rate of turbulent kinetic energy (ε) (m2s-3)

$$\frac{\partial \varepsilon}{\partial t} + u_j \frac{\partial \varepsilon}{\partial x_j} = \frac{1}{\rho}\frac{\partial}{\partial x_j}\left[\left(\mu + \frac{\mu_t}{\sigma_\varepsilon}\right)\frac{\partial \varepsilon}{\partial x_j}\right] + C_1 S\varepsilon - C_2 \frac{\varepsilon^2}{k + \sqrt{\nu\varepsilon}}$$

The Reynolds stress is:

$-(\overline{u_i' u_j'}) = \frac{1}{\rho}\mu_t\left(\frac{\partial u_i}{\partial x_j} + \frac{\partial u_j}{\partial x_i}\right) - \frac{2}{3}k\delta_{ij}$, where $\mu_t = \rho\frac{C_\mu k^2}{\varepsilon}$ is the turbulent viscosity; where C_μ is a model constant which is not fixed.

$$C_\mu = \frac{1}{A_0 + A_s(kU^*/\varepsilon)}, \text{ where } A_0 = 4.04,$$

$$A_s = \sqrt{6}\cos\phi,$$

$$\phi = \frac{1}{3}\left(\cos^{-1}\left(\sqrt{6}W\right)\right),$$

$$W = S_{ij}S_{jk}S_{ki}/\tilde{S}^3,$$

$$\tilde{S} = \sqrt{S_{ij}S_{ij}},$$

$$S_{ij} = \frac{1}{2}\left(\left(\partial u_j/\partial x_i\right) + \left(\partial u_i/\partial x_j\right)\right),$$

$U^* = \tilde{S} = \sqrt{S_{ij}S_{ij}}$ (Where there is no rate of rotation in the stationary reference frame for this study).

Legend:

u_j = j component of *mean* velocity (ms^{-1});

u_j' = root-mean-square of the velocity fluctuation j component;

P = pressure in Newton per meter square (Nm^{-2});

t = time in seconds (s);

x_j = j coordinate (m);

ρ = air density (kgm^{-3});

μ = dynamic (molecular) viscosity ($kgm^{-1}s^{-1}$);

g_i = gravitational body force (ms^{-2});

G_k = turbulent kinetic energy production ($kgm^{-1}s^{-2}$);

S = scalar measure of deformation or mean strain rate (m^2s^{-2});

ν = molecular kinematic viscosity (μ/ρ);

Constants:

σ_k = 1.0 (Turbulent Prandtl number for *k*);

σ_ε = 1.2 (Turbulent Prandtl number for ε);

C_1 = $\max\left[0.43, \frac{\eta}{\eta+5}\right]$, where $\eta = Sk/\varepsilon$, where $S = \sqrt{2S_{ij}S_{ij}}$ is the scalar measure of the deformation tensor;

C_2 = 1.9.

Previous researchers' studies showed that the RLZ model performs best in separated flows and flows with complex secondary flow, provided that it is properly coupled with a two-layer all y^+ wall treatment near the 'wall' boundary condition [25, 27, 28]. The RLZ turbulence model has also shown superiority in modeling flows that include boundary layers under strong adverse pressure gradients, separation and recirculation as compared to other RANS models [25, 28] and excels at modeling flow that involves high shear or separation commonly encountered in buildings simulation [29]. The two-layer zonal model treatment that is used together with this model provides improved convergence, requires less mesh elements in the viscosity sub-layer and introduces proper distribution of the turbulent length scale near the walls [30, 31]. All the simulation cases are carried out under steady state fluid flow and isothermal conditions. Air within the domain is regarded as incompressible turbulent inert flow which is according to the assumption that at low subsonic speeds, air densities are considered constant under varying pressures for lower atmospheric environment as described by Sini et al. [15].

C. Computational Domain and Mesh Type

The computational domain adopted here consists of a large cylindrical atmospheric volume of radius 1800m and height of 800m, similar to the one proposed by Lee et al. as shown in Fig. 13 [32]. The middle portion of this atmospheric domain consists of the HDB blocks whereby the parametric study of morphological variations will be carried out. The domain radius is 3 times of the longest distance length of the development from the development boundary to the domain edge [33]. The domain height extends 6 times the tallest building's height from the top of the highest building in the whole development to the top of the domain [34]. We used the height of the point blocks (112m), which are taller compared to the slab blocks (50m). Both requirements are the most stringent among those suggested by most researchers and guidelines.

Unstructured polyhedral grids with a growth factor of 0.9 are generated for the whole computational domain with localized mesh size of the blocks set at 1.2m. Wind from different orientations will be simulated with the same cylindrical domain (Fig. 13). The curved inlet boundary acts as the inflow of winds from different orientations (0˚, 22.5˚, 45˚, 67.5˚ and 90˚ north). The cylindrical top is a symmetry plane (slip wall condition) and the cylinder bottom (non-slip wall condition) is where the power-law wind profile will move in from the inlet before arriving at the estate area. The outlet is considered to be the opposite side of the wind orientation.

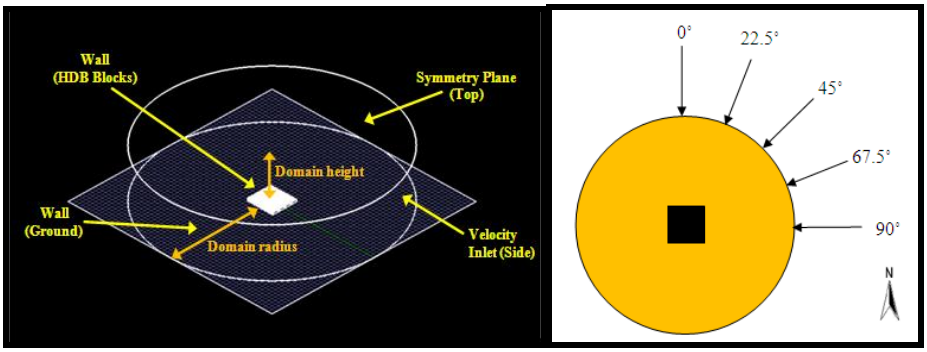

Fig. 13 Computational domain and wind orientations from north; the middle estate area of 500×500m will be subjected to various morphological variations [32]

D. Boundary Conditions

A power-law wind profile is generated (using BCA's Code for Environmental Sustainability of Buildings, 2nd Edition), averaged at 2.7m/s from all the four prevailing wind directions (at reference height of 15.00m) [33] (Table 3). The other input variables are the same with the ones that is used by Lee et al., as shown in Table 4 [32].

TABLE 3 TABULATION OF PREVAILING WIND DIRECTION AND SPEED OBTAINED FROM NEA (NATIONAL ENVIRONMENT AGENCY) OVER A PERIOD OF 18 YEARS [33]

Wind Direction	Mean Speed (m/s)
North	2.0
North-east	2.9
South	2.8
South-east	3.2

TABLE 4 IMPUT VARIABLES FOR THE INLET BOUNDARY CONDITIONS [32]

Parameter	Value	Input	Researcher
Power law exponent (α)	α = 0.21 [35].	Power law – to approximate the vertical upwind profile flow in medium density suburban areas. Ensuring that the minimum threshold speeds of 2m/s for development of canyon vortices observed by DePaul and Shieh was comfortably exceeded.	De Paul and Shieh, 1986 [37]
Roughness length (Z_0)	$Z_0 = 0.5$ (Suburban terrains, forest, regular large obstacles, etc). [36]		
Turbulence intensity (Ti)	5% (low speed flows for ventilation)		
Turbulent kinetic energy (*k*)	At Ti =5%, occurs at H = 467m above ground of the power-law wind profile worked out. Wind velocity at this height is Ur = 5.56m/s [35].	$k = \frac{3}{2}(U_r T_i)^2$ Where Ti represents the turbulence intensity, Ur is the reference velocity at the level where Ti = 5%.	
Turbulent dissipation (ε)		$\varepsilon = \frac{C_\mu^{3/4} k^{3/2}}{l}$ Empirical constant Cμ = 0.09 and l = 0.07L, where L is the characteristic length and in this case, the longest distance measured across each estate. I.e. the length of the estate = 500m.	
Von Karman constant	K = 0.41 (urban areas)		

E. Model Validation (Wind Tunnel Test)

Wind tunneling modeling is used for the verification study of the Star-CCM+ software. Physical scale models to be tested were constructed and placed in an open circuit boundary-layer wind tunnel (BLWT) at the National University of Singapore. The wind tunnel dimensions are at a length of 21.00m (original length is 17m, now extended by another 4m) by a width of 3.75m by a height of 1.75m [38]. The test section where the model is placed contains a large turntable that is used to vary the wind direction relative to the model.

A constant power-law wind profile is generated to be as the closest possible to the one that is used in this CFD parametric study, which is based on 2.7m/s at reference height of 15m (in prototype case), with the power law coefficient of α = 0.21 (based on roughness length Z_0 = 0.5). This reference wind speed and height is derived from the average speed of the four prevailing wind directions (north, northeast, south and southeast) in Singapore taken over a period of 18 years [33] as shown in Table 3. The maximum speed at a reference height altitude is measured or estimated and the boundary layer is structured according to $\frac{U}{U_{ref}} = \left(\frac{Z}{Z_{ref}}\right)^{\alpha}$ where U = mean velocity at height z, U_{ref} = mean velocity at reference height Z_{ref} [39]. The geometric scale of the model of a building or structure should be chosen to maintain, as closely as possible, the equality of model and prototype ratios of overall building dimensions to the important meteorological lengths of the modeled approach wind [40]. The next issue to consider is the scale of the model which is related to the Reynolds number scaling. Fortunately for most non-curved structures such as ordinary buildings, it is not necessary to use the prototype Reynolds number $\mathrm{Re}_b = \frac{V_h L_b}{\nu}$ for wind tunnel tests. V_h is the velocity of wind at the location, L_b is the characteristic overall dimension of a building and ν = kinematic viscosity of air. As long as the Reynolds number for the model is not too small (at least 10^4), the flow around the model will be turbulent, and kinematic and dynamic similarities will prevail even if the model's Reynolds number is much smaller than the prototype Reynolds number [40-42]. The scale of the model used here is 1:400 and the Reynolds number calculated from it has already far exceeded the minimum required value of 10^4.

In the wind profile similar to that in CFD study, the wind velocities measured can be used for validation purposes. The tests were carried out over a range of wind directions varying from - 0˚, 22.5˚ to 45˚ for point blocks and from 0˚, 45˚ to 90˚ for slab blocks. The scale models were subjected to a controlled wind flow and velocity readings at each sensor tap corresponds to the velocity at the particular location at pedestrian-level (2m above ground in prototype case) and mid-levels (56m for point blocks, 25m for slab blocks). Velocities were measured using the Dantec metal-clad probe at the measuring locations indentified by their position number as shown in the Fig. 14. It consists of a wire-wound sensor protected by a thin-walled nickel tube, mounted on a 2mm thick plate equipped with a two-pole connector. The probe voltage is converted to wind velocity after corrected for variations in air temperature. The mean time velocities were determined by averaging the instantaneous velocities sampled over 3 minutes at 2s frequency.

The results of the velocity magnitude are as shown in Fig. 15 for point blocks and Fig. 16 for slab blocks. The results show a fairly good agreement between both wind tunnel readings and CFD readings with a margin of difference of 0.50m/s between most readings, even though there are some signs of under-prediction by the CFD results for readings at the side areas.

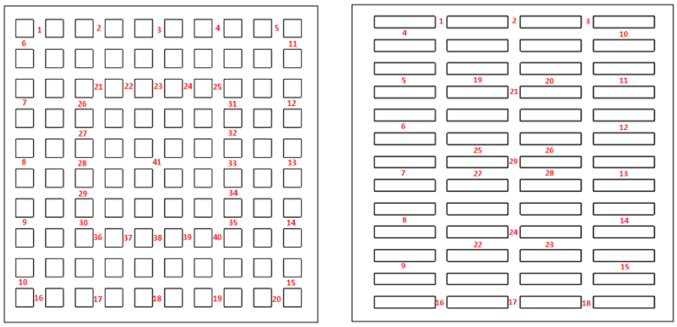

Fig. 14 Sensor Probe Positions for Point Blocks (Left) and Slab Blocks (Right)

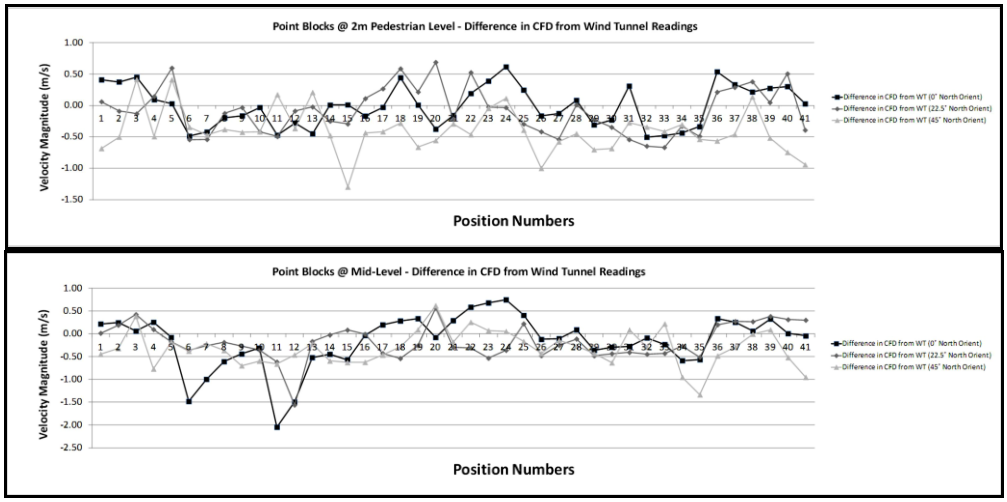

Fig. 15 Comparison of CFD and wind tunnel readings for point blocks at pedestrian and mid-level

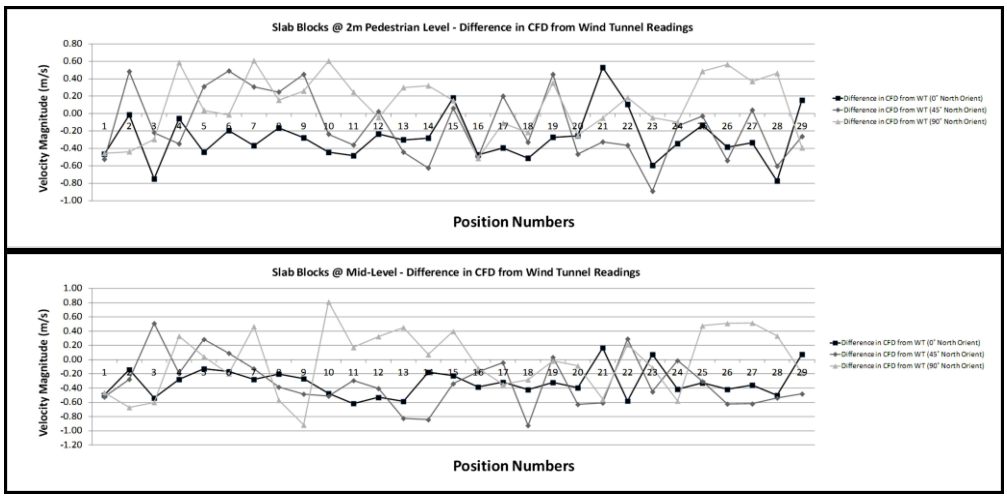

Fig. 16 Comparison of CFD and wind tunnel readings for slab blocks at pedestrian and mid-level

F. Wind Velocity Ratio (V_R)

The wind velocity ratio (V_R) is used as an indicator of testing good ventilation in this study. It is measured and defined as $V_R = V_p / V_\infty$, where V_∞ is the wind velocity at the top of an UBL not affected by the ground roughness, buildings and local site features (typically assumed to be at a certain height above the roof tops of the area and is site dependent) [43]. V_P is the wind velocity at pedestrian level (2m above ground) after taking into account the effects of buildings. V_R indicates how much of the wind availability of a location could be experienced by pedestrians near the ground taking account of the surrounding buildings. The concept of V_R can also be used for other measured levels besides pedestrian level.

Lee et al. mentioned that according to the incoming Singapore power-law wind profile as mentioned in the section on 'Boundary Conditions', V_∞ will be fixed (for all V_R calculations) at a certain height above ground [32]. This height level is where the change in incoming wind velocity between the selected level (1m interval between each level) and the cylindrical domain top that is assumed to be at 800m above ground has a difference of 1% or less.

It is worked out as follows according to the wind profile of $\alpha = 0.21$:

Top of domain (800m above ground) = 6.22m/s

745m above ground = 6.13m/s

Difference between both levels = (6.22 – 6.13) m/s

= 0.09m/s (≈ 1% difference)

Hence, V_∞ as 6.13m/s is used for working out the V_R. The area-averaged outdoor velocity magnitude values for V_P will be extracted at the pedestrian-level (2m above ground level) and the mid-level (56m for point blocks and 25m for slab blocks) and area-averaged (according to cell size) within a constrained horizontal plane that is confined within the precinct area (500m by 500m).

IV. RESULTS AND DISCUSSION

A. Point Block, Pedestrian Level

The overall results for area-averaged V_R values within the estate for point blocks under the random, group and courtyard GBCR configurations are shown in Fig. 17 for pedestrian level.

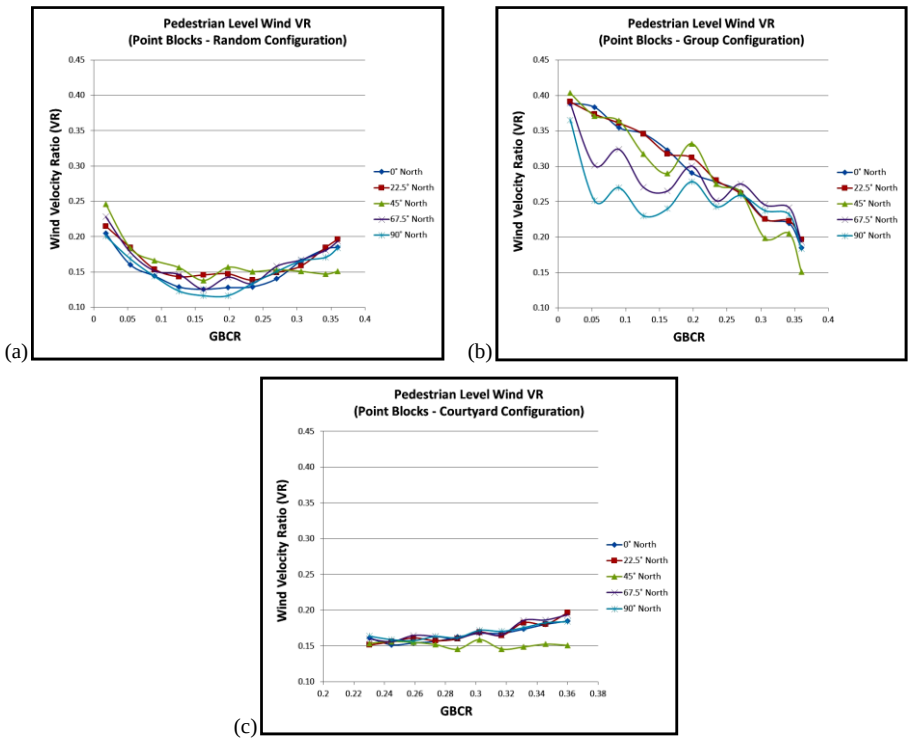

Fig. 17 Pedestrian level area-averaged V_R against GBCR for (a) random, (b) group and (c) courtyard configuration of point blocks

1) Point Blocks, Pedestrian Level - Random Configuration:

From the parametric study results, V_R for all wind directions, except 45˚ north, follow a hump shape. As GBCR increases, V_R decreases and then up to a point at around 0.162, V_R increases (Fig. 17a). The reason is that during the first half of the studies (GBCR values from 0.000 to 0.162), as GBCR increases, the increased number of point blocks significantly increases the ground roughness (Figs. 18a and 18b). Therefore, the frictional effects to the airflow increases, leading to a decrease in V_R. This phenomenon continues until a point in time that further GBCR increase causes more buildings to be placed close to each other and form very effective canyons. This increase in canyon numbers gives rise to more channeling effects that helps to increase the wind speed for the whole precinct at the pedestrian level (Figs. 18c and 18d). As for winds from 45˚ north, due to the wind direction, wind flows within the main canyons from both transverse directions are equally opposing and hence, the roughness that comes from GBCR effect (increase in buildings) is greater than the channeling effect that happens in the other directions (Figs. 18e and 18f). That is why we see a decreasing V_R curve with decreasing gradient (reverse natural logarithm) as GBCR increases, agreeing with the common notion from previous researchers that increasing GBCR gives you decreasing wind speed.

Next, we observed that the other wind directions like 22.5˚, 45˚ and 67.5˚ north have slightly higher speeds than 0˚ and 90˚ north winds. The reason is during the increase in GBCR, there are no clear straight canyons initially and it is towards the higher GBCR ratios that canyons started to form. Hence, throughout the whole process, the so-called channeling effect (which commonly gives higher velocity readings for canyons that are parallel to wind orientation in general) that we are so familiar with did not take place. Furthermore, oblique wind flow in random cases helps to provide more incoming wind from canyon intersections in both directions versus winds that are coming from 0˚ and 90˚ north which may encounter blockages from frontal buildings.

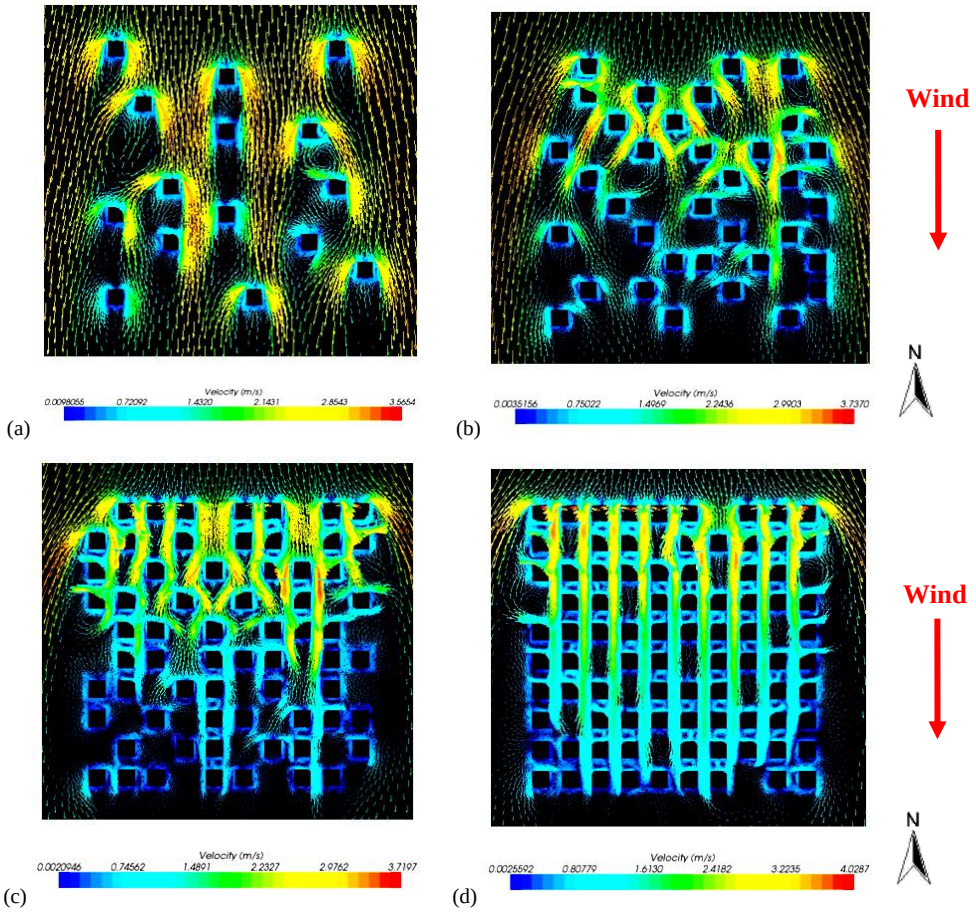

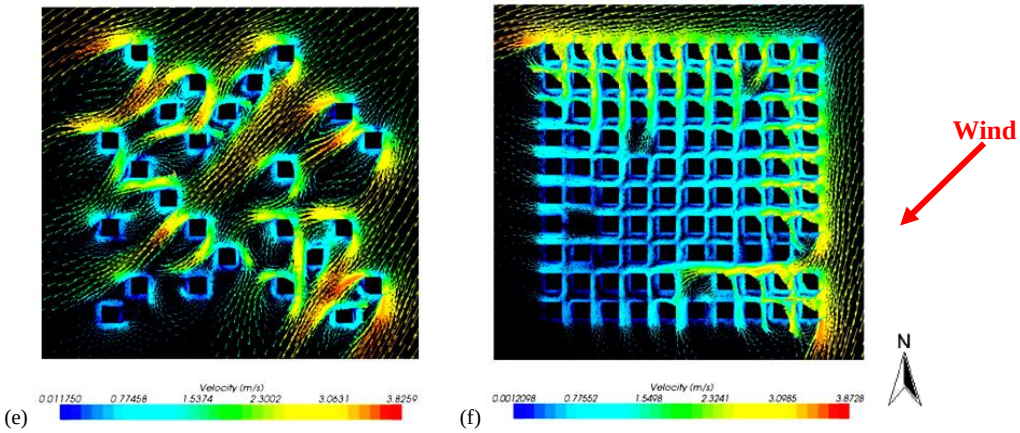

Fig. 18 Point blocks, random configuration:

(a) Velocity vectors for GBCR = 0.054 for wind from 0˚ north (pedestrian level)
(b) Velocity vectors for GBCR = 0.126 for wind from 0˚ north (pedestrian level)
(c) Velocity vectors for GBCR = 0.234 for wind from 0˚ north (pedestrian level)
(d) Velocity vectors for GBCR = 0.306 for wind from 0˚ north (pedestrian level)
(e) Velocity vectors for GBCR = 0.090 for wind from 45˚ north (pedestrian level)
(f) Velocity vectors for GBCR = 0.342 for wind from 45˚ north (pedestrian level)

2) Point Blocks, Pedestrian Level - Group Configuration:

The results show generally higher V_R values compared to that of the random configuration (Figs. 17a and 17b). This is due to the increased in full empty spaces as all buildings are now grouped together and at the same time, the formation of relatively more canyons (due to the grouping) for the channeling effects to take place. These groupings of buildings have also resulted in a general decrease in V_R as GBCR increases, as it is a straight forward consideration of building footprint coverage that is different the random configuration (Figs. 19a and 19b).

Next, the difference in V_R readings between 0˚ and 90˚ north orientation and between 22.5˚ and 67.5˚ north orientation readings is due to the location of the chunk of empty space. E.g. if the empty space is in front-most towards the wind direction, readings at this area are very high. If the same empty space is at back of precinct (away from the approaching wind), wind flow will be much lower due to the buildings blocking in front. But nevertheless, the decreasing trend is still discernible. Furthermore, we also see that as GBCR increases, the differences in V_R between 0˚ and 90˚ north, and 22.5˚ and 67.5˚ decreases. As more and more spaces are being occupied with buildings as GBCR increases, the effect of an uneven distribution of empty spaces is being minimized.

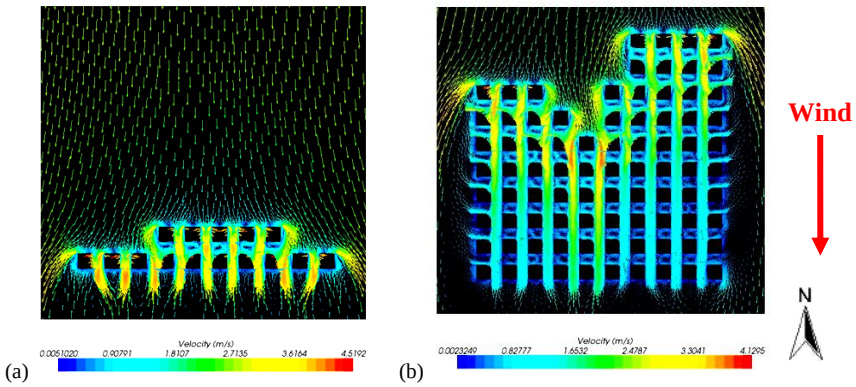

Fig. 19 Point blocks, group configuration:

(a) Velocity vectors for GBCR = 0.054 for wind from 0˚ north (pedestrian level)
(b) Velocity vectors for GBCR = 0.306 for wind from 0˚ north (pedestrian level)

3) Point Blocks, Pedestrian Level - Courtyard Configuration:

The results show generally lower V_R readings than the group configuration (Figs. 17b and 17c). This is due to the enclosed precinct that has buildings bordering around the perimeter that act as blockages. This reduces the amount of wind entering into a precinct as compared to a group configuration which does not have this problem. On the other hand, the V_R readings are quite comparable to the random configuration (Figs. 17a and 17c). This is due to the courtyard configuration having more lumps of empty spaces and also the offsetting effects of their surrounding blockages. This is balanced by the random configuration which does not have blockages surrounding their precinct but is offset by their broken up empty spaces (which contributed to roughness) as compared to the courtyard configuration. Readings from the courtyard configurations are slightly

higher at the first part of GBCR (0.230 to 0.288) compared to random configuration. This could be due to the broken up empty spaces in random configuration contributing to the roughness and subsequently as GBCR increases, the difference tends to diminish as just mentioned. The other observation is the general increase in V_R with GBCR increment. This is a result of the increase in number of canyons for the channeling effects, while having the same precinct border lined up with point blocks (Figs. 20a and 20b).

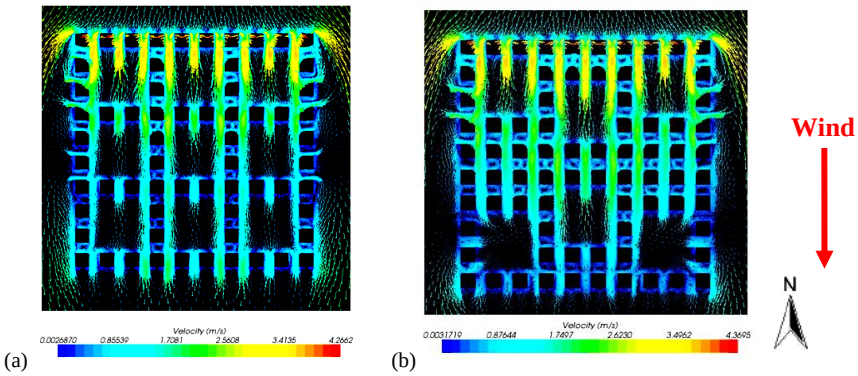

Fig. 20 Point blocks, courtyard configuration:

(a) Velocity vectors for GBCR = 0.230 for wind from 0˚ north (pedestrian level)
(b) Velocity vectors for GBCR = 0.274 for wind from 0˚ north (pedestrian level)

B. Point Block, Mid-Level

The overall results for area-averaged V_R values within the estate for point blocks under the random, group and courtyard GBCR configurations are shown in Fig. 21 for mid-level.

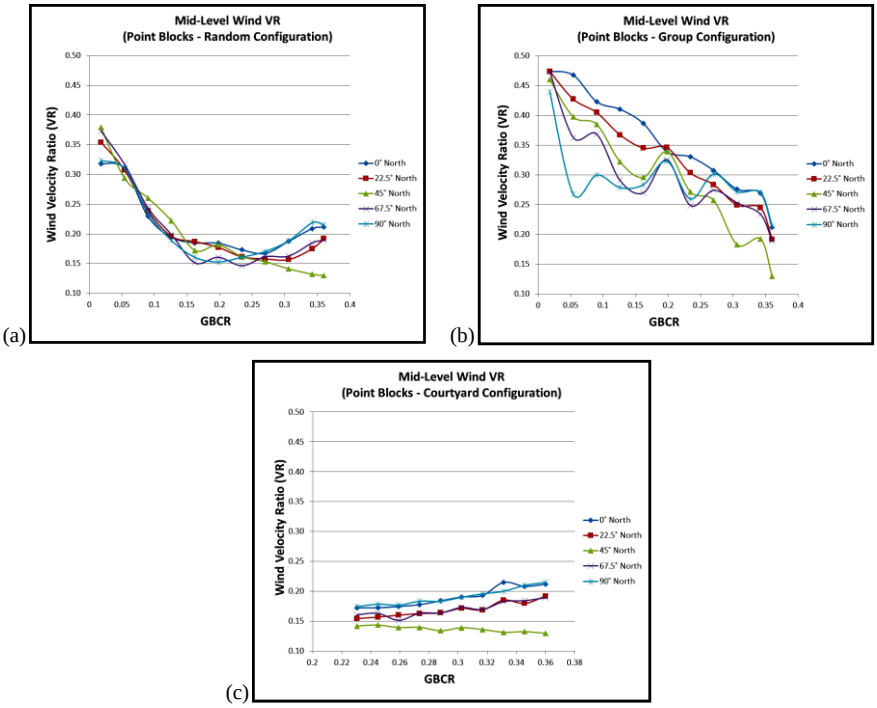

Fig. 21 Mid-level area-averaged V_R against GBCR for (a) random, (b) group and (c) courtyard configuration of point blocks

1) Point Blocks, Mid-Level - Random Configuration:

In GBCR random configuration for point blocks at mid-level, the behavioral patterns and the reasons behind are very similar to that of the configuration at pedestrian level (Figs. 17a and 21a). Generally, the V_R readings for mid-levels are higher than pedestrian level due to the stronger wind flow at upper levels. Next, it is observed that as GBCR increases, V_R decreases and then up to a point at around 0.234, V_R increases i.e. following a hump shape. The reason is during the first half of the studies (GBCR values from 0.000 to 0.234), as GBCR increases, the increased number of point blocks significantly increases the ground roughness. Therefore, the frictional effects to the airflow increases, leading to a decrease in V_R (Figs. 22a and 22b). This phenomenon continues till a point in time that further increase in GBCR allows more buildings to be placed close to each other which help to form very effective canyons. This increase in canyon numbers gives rise to more channeling effects that

increases mid-level wind speeds for the whole precinct (Figs. 22c and 22d). As for the V_R readings for the 45˚ north wind orientation, it follows a decreasing V_R curve with decreasing gradient (reverse natural logarithmic curve) as GBCR increases. The reasons behind all these mid-level behavior are generally similar to the cases for ***Point Blocks, Pedestrian Level - Random Configuration***.

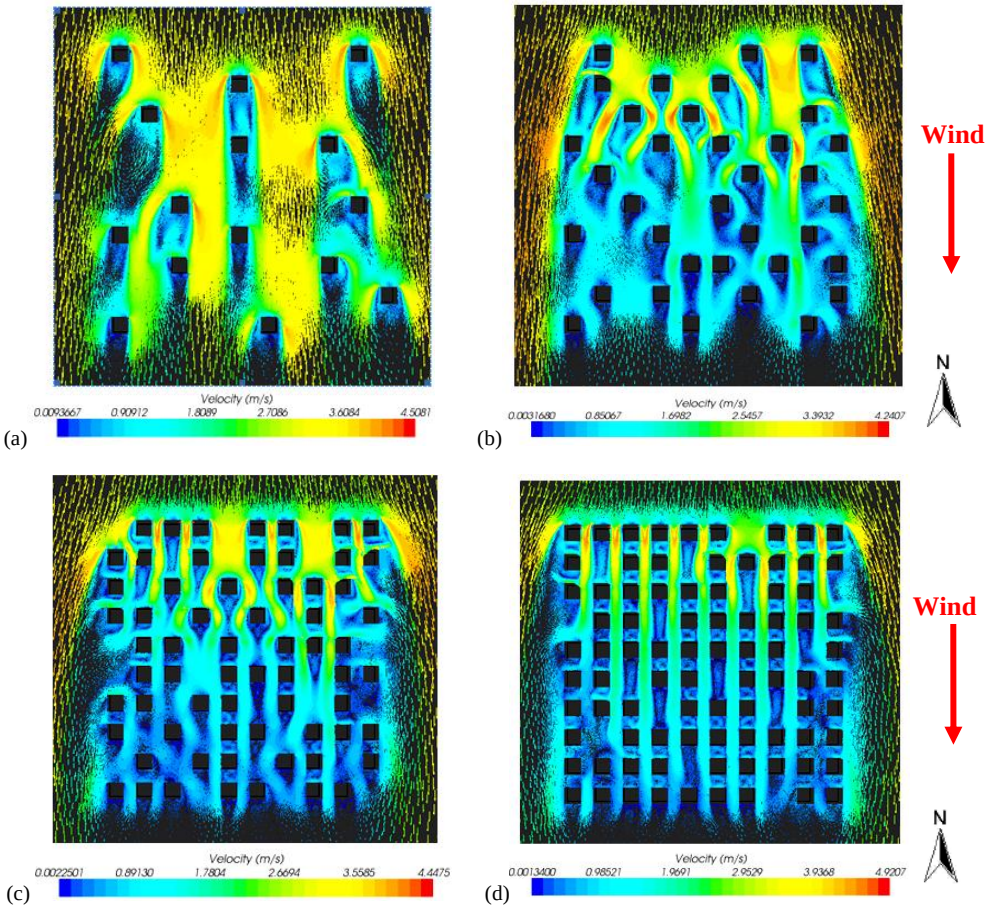

Fig. 22 Point blocks, random configuration:

(a) Velocity vectors for GBCR = 0.054 for wind from 0˚ north (mid-level)
(b) Velocity vectors for GBCR = 0.126 for wind from 0˚ north (mid-level)
(c) Velocity vectors for GBCR = 0.234 for wind from 0˚ north (mid-level)
(d) Velocity vectors for GBCR = 0.306 for wind from 0˚ north (mid-level)

2) Point Blocks, Mid-Level - Group Configuration:

In GBCR group configuration for point blocks at mid-level, the behavioral patterns and the reasons behind are very similar to the same configuration at pedestrian level (Figs. 17b and 21b). Generally, the V_R readings for mid-levels are higher than pedestrian level due to the stronger wind flow at upper levels. The main features observed here are higher V_R values as compared to the random configuration at mid-level (Figs. 21a and 21b) and the decrease in V_R readings as GBCR increases. The explanations are similar to the cases in ***Point Blocks, Pedestrian Level - Group Configuration***. Fig. 23 shows the vector diagrams for mid-level group configurations where we can see the groupings of buildings have resulted in a general decrease in V_R as GBCR increases. It is a straight forward consideration of building footprint coverage in this case (Figs. 23a and 23b).

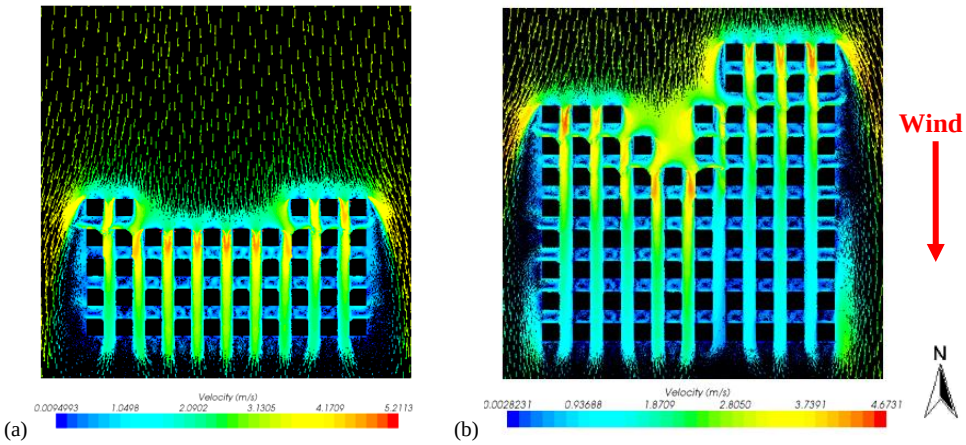

Fig. 23 Point blocks, group configuration:

(a) Velocity vectors for GBCR = 0.162 for wind from 0˚ north (mid-level)
(b) Velocity vectors for GBCR = 0.306 for wind from 0˚ north (mid-level)

3) Point Blocks, Mid-Level - Courtyard Configuration:

In GBCR courtyard configuration for point blocks at mid-level, the behavioral patterns and the reasons behind are very similar to the same configuration at pedestrian level (Figs. 17c and 21c). Generally, the V_R readings at mid-levels for all orientations, except 45˚ north, are higher than pedestrian level due to the stronger wind flow at upper levels. The reason for lower mid-level V_R readings than pedestrian level for wind from 45˚ north orientation is the opposing wind flows within the main canyons from both transverse directions. Furthermore, it is more prone to disturbance from higher turbulence at mid-levels compared to that of pedestrian level. Wind flow at pedestrian level is generally more orderly and not being disturbed as much as that at mid-levels. It is this disturbance from higher turbulence that causes the wind to be further slowed down compared to pedestrian level. This phenomenon affects the courtyard configuration more than the others because of the surrounding blockages in the precinct.

The other main features observed at mid-level are lower V_R values as compared to the group configuration (Figs. 21b and 21c), comparable V_R readings to the random configuration (Figs. 21a and 21c) and increase in V_R as GBCR increases (except 45˚ north wind orientation cases). The explanations are similar to the cases in ***Point Blocks, Pedestrian Level – Courtyard Configuration***. As for the slight decreasing trend with GBCR increase for 45˚ north wind orientation cases at mid-level, it could be due to the opposing wind flow within the main canyons from both transverse directions whereby the channeling effects do not come into play as in other wind orientations. Furthermore, the presence of higher turbulence found at higher levels within the UCL manifest this decreasing trend as compared to pedestrian level which has a more constant gradient due to lesser turbulence. Fig. 24 shows the vector diagrams for mid-level courtyard configurations where we can see the stronger wind channeling effects when GBCR is 0.274 (Fig. 24b) compared to when 0.230 (Fig. 24a) for 0˚ north wind orientation.

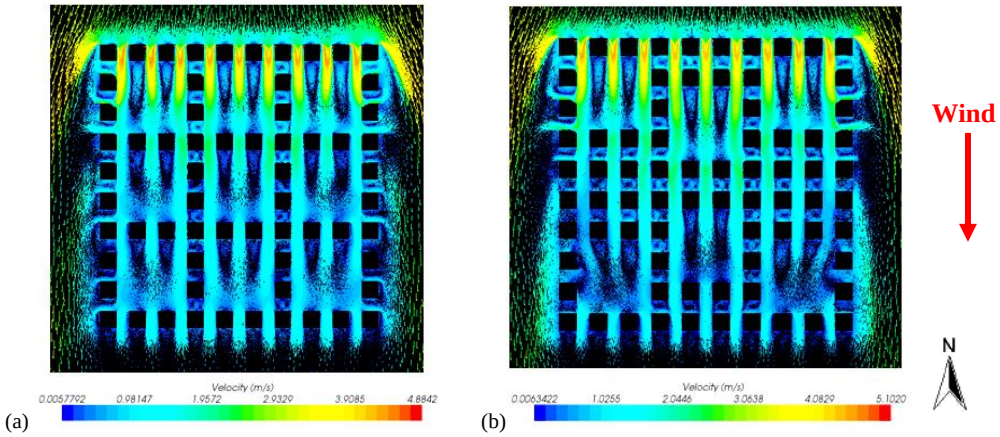

Fig. 24 Point blocks, courtyard configuration:

(a) Velocity vectors for GBCR = 0.230 for wind from 0˚ north (mid-level)
(b) Velocity vectors for GBCR = 0.274 for wind from 0˚ north (mid-level)

C. Slab Blocks, Pedestrian Level

The overall results for area-averaged V_R values within the estate for slab blocks under the random, group and courtyard GBCR configurations are shown in Fig. 25 for pedestrian level.

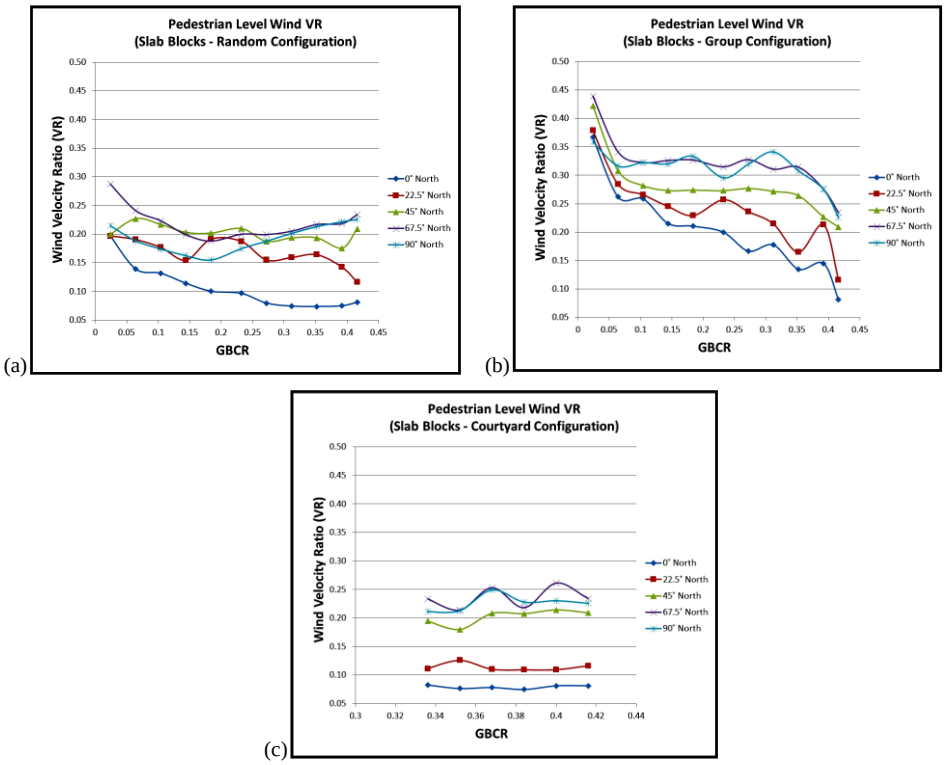

Fig. 25 Pedestrian level area-averaged V_R against GBCR for (a) random, (b) group and (c) courtyard configuration of slab blocks

1) Slab Blocks, Pedestrian Level - Random Configuration:

The results show that V_R readings for wind directions like 0˚ and 22.5˚ north tend to decrease as GBCR increases (Fig. 25a). On the other hand, for wind directions like 67.5˚ and 90˚ north, it follows a hump shape whereby as GBCR increases, V_R decreases up to a point (GBCR value of around 0.184) and then starts to increase again. For 0˚ and 22.5˚ north wind orientations, this behavior is due to the fact that for the number of canyons that are parallel to (0˚ north) or slightly oblique to the wind orientation (22.5˚ north), there are only three of them (Figs. 26a and 26b). Hence, this arrangement tends to be more affected by the building footprint GBCR value, thereby leading to the decrease in V_R as GBCR increases. The change in the number of canyons by varying the GBCR value does not help to create more canyons for channeling effects as in the case for point blocks. For 67.5˚ and 90˚ north wind orientations, the number of canyons that are parallel to (90˚ north) or slightly oblique to the wind flow (67.5˚ north), there are twelve of them which is much more. This gives rise to the possibility that during the first half of GBCR until around 0.184, the increased number of slab blocks significantly increases the ground roughness, therefore leading to a decrease in V_R (Fig. 26c). This phenomenon continues until a point that further increase in slab blocks placed close to each other forms very effective canyons that help to advance the channeling effects in the whole precinct (Fig. 26d). This helps to increase V_R at pedestrian level from 0.184 till 0.416.

For winds coming from 45˚ north, there is a decreasing trend for V_R readings which is much more gradual. The reason for this is that winds from 45˚ north have equally opposing wind flow within the precinct from both transverse main canyon directions. Hence, ground roughness that comes from the GBCR increase exerts a greater effect than the channeling effects that are seen in other orientations with higher number of canyons parallel to the wind flow.

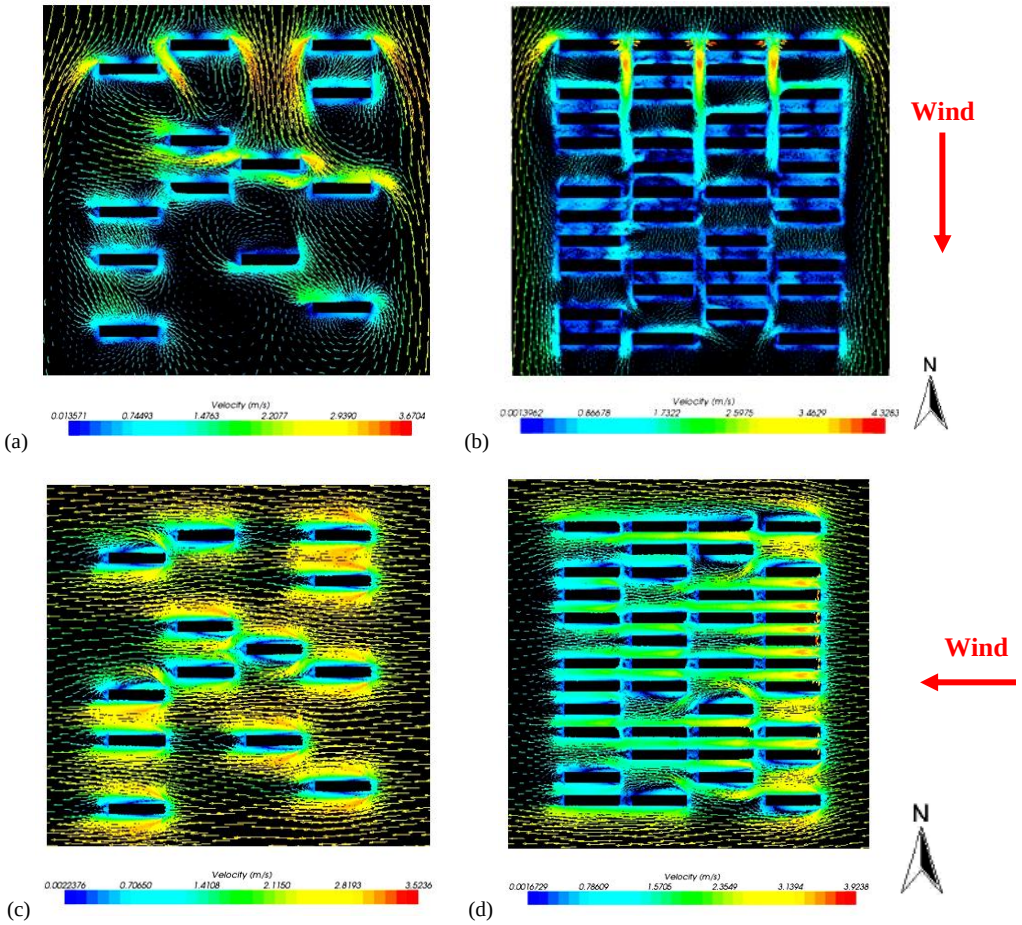

Fig. 26 Slab blocks, random configuration:

(a) Velocity vectors for GBCR = 0.104 for wind from 0˚ north (pedestrian level)
(b) Velocity vectors for GBCR = 0.312 for wind from 0˚ north (pedestrian level)
(c) Velocity vectors for GBCR = 0.104 for wind from 90˚ north (pedestrian level)
(d) Velocity vectors for GBCR = 0.312 for wind from 90˚ north (pedestrian level)

2) Slab Blocks, Pedestrian Level - Group Configuration:

The V_R readings in group configurations are generally higher if compared to the random configuration (Figs. 25a and 25b). This is due to the increased in full empty spaces as all buildings are now grouped together and at the same time, the formation of relatively more canyons (due to the grouping) for the channeling effects to take place. The study also shows that for all wind orientations, there is a general decrease in V_R as GBCR increases. The reason is that when buildings are grouped together, the increased in GBCR plays an important role in increasing the surface roughness of the ground within the precinct. It is a straight forward consideration of building footprint coverage unlike the random configuration. But this decreasing trend seems to decrease in gradient when wind orientation goes from 0˚ to 90˚ north. This indicates the decrease in roughness influence of GBCR manifests when wind orientation changes from 0˚ north to 90˚ north. The least influence of GBCR on winds from 90˚ north is because for slab blocks, the cross section wall area facing the wind is least (hence more canyons) (Figs. 27a and 27b), thereby resulted in less massive blockages compared to wind from 0˚ north. The 0˚ north wind is blocked by more surface wall area facing the wind direction and this causes the GBCR to have a larger influence on overall V_R values (Figs. 27c and 27d).

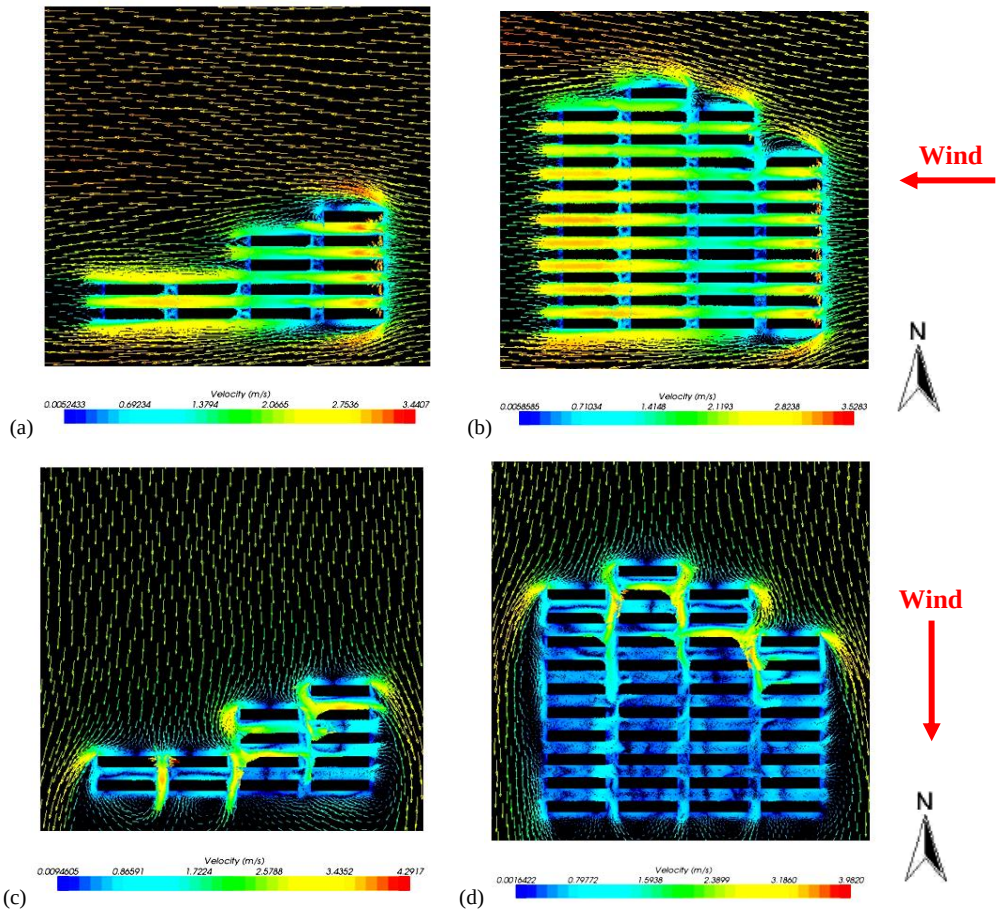

Fig. 27 Slab blocks, group configuration:

(a) Velocity vectors for GBCR = 0.104 for wind from 90˚ north (pedestrian level)
(b) Velocity vectors for GBCR = 0.312 for wind from 90˚ north (pedestrian level)
(c) Velocity vectors for GBCR = 0.104 for wind from 0˚ north (pedestrian level)
(d) Velocity vectors for GBCR = 0.312 for wind from 0˚ north (pedestrian level)

3) Slab Blocks, Pedestrian Level - Courtyard Configuration:

The V_R readings are generally lower than the group configuration (Figs. 25b and 25c). This is due to the enclosed precinct that has buildings bordering around the perimeter. They act as blockages which reduce the amount of wind entering into a precinct as compared to a group configuration which do not have this problem. Next, there is a general increase in V_R as GBCR increases which is due to the increase in canyon numbers for the channeling effects, while having the same precinct border lined up with slab blocks. As wind orientation changes from 0˚ to 90˚ north, the gradient of the trend increases. This is due to the increase in channeling effects, especially for wind orientation cases that have more canyons parallel to it and smaller influence of the massive wall surfaces against the wind (e.g. 90˚ north orientation) (Figs. 28a and 28b). The higher the number of canyons parallel to the wind orientation i.e. 67.5˚ or 90˚ north, the steeper is the gradient of increase with increasing GBCR because of higher channeling effects. The oscillating readings of 67.5˚ north and 90˚ north could be due to the positions of the courtyard as sometimes the empty spaces may act as diffusion areas if placed towards the wind direction. If this is placed at the back away from wind direction, the canyons in front will have ample channeling effect in place and hence, will give an overall higher V_R. Next, the higher the number of canyons towards the wind orientation (e.g. 67.5˚ and 90˚ north wind orientations), the higher is the V_R at the same level. It is because there are higher numbers of channels in place compared to the extreme case of 0˚ north that have more massive wall surfaces facing the wind (Figs. 28c and 28d).

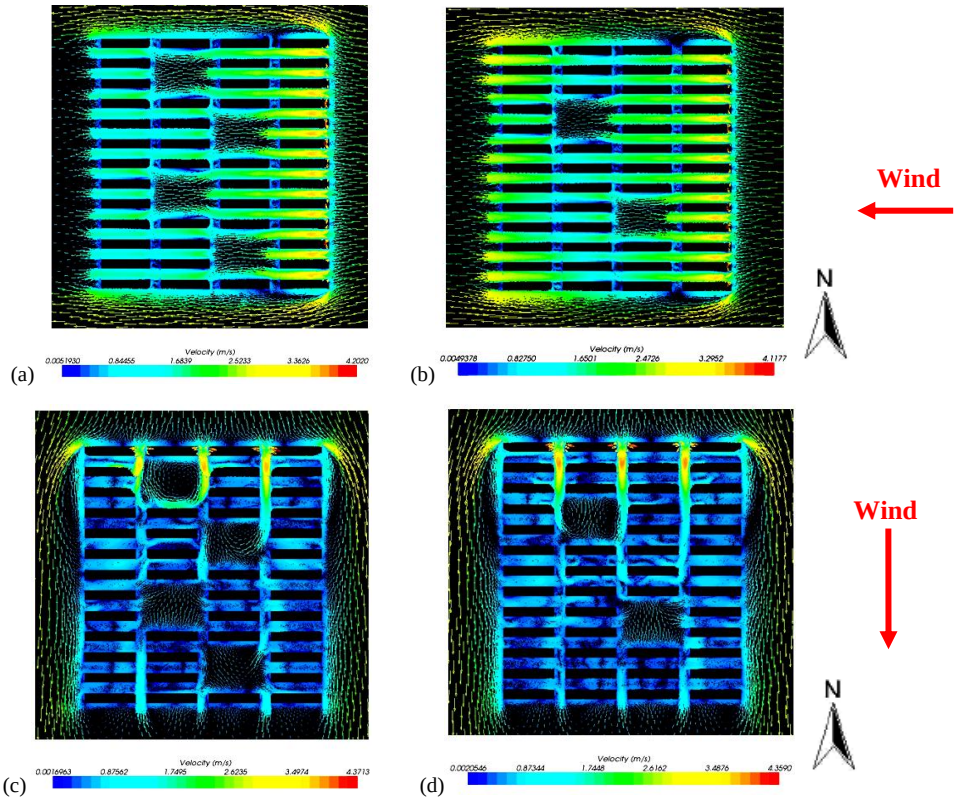

Fig. 28 Slab blocks, courtyard configuration:

(a) Velocity vectors for GBCR = 0.352 for wind from 90˚ north (pedestrian level)
(b) Velocity vectors for GBCR = 0.384 for wind from 90˚ north (pedestrian level)
(c) Velocity vectors for GBCR = 0.352 for wind from 0˚ north (pedestrian level)
(d) Velocity vectors for GBCR = 0.384 for wind from 0˚ north (pedestrian level)

D. Slab Blocks, Mid-Level

The overall results for area-averaged V_R values within the estate for slab blocks under random, group and courtyard GBCR configurations are shown in Fig. 29 for mid-level.

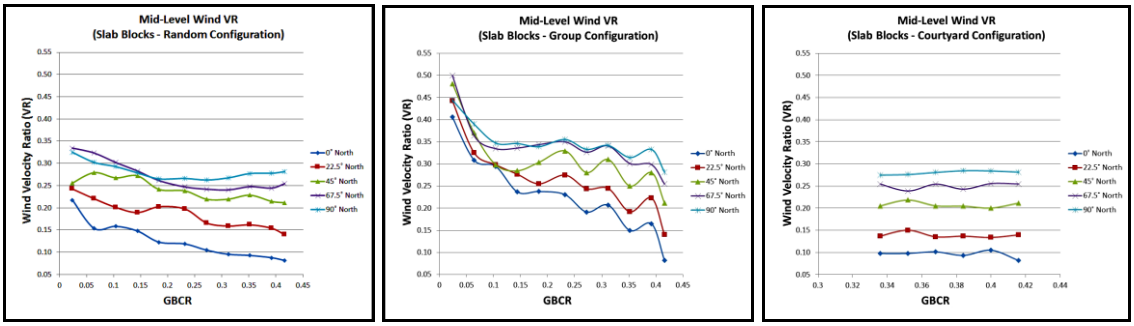

Fig. 29 Mid-level area-averaged V_R against GBCR for (a) random, (b) group and (c) courtyard configuration of slab blocks

1) Slab Blocks, Mid-Level - Random Configuration:

In GBCR random configuration for slab blocks at mid-level, the V_R values are generally higher than those from pedestrian level due to the stronger wind at upper levels (Figs. 25a and 29a). The rest of the behavioral patterns and the reasons behind are similar to the same configuration at pedestrian level. Some of these behavioral patterns include the decrease in V_R readings with GBCR increase for 0˚ and 22.5˚ north wind orientation cases; V_R readings following a hump shape in 67.5˚ and 90˚ north wind orientation cases whereby as GBCR increases, V_R decreases up to a point (around GBCR of 0.272) and then starts to increase again, and lastly the gradual decrease in trend for V_R readings with GBCR increase for 45˚ north wind orientation cases.

2) Slab Blocks, Mid-Level - Group Configuration:

In GBCR group configuration for slab blocks at mid-level, the V_R values are generally higher than those from pedestrian level due to the stronger wind at upper levels (Figs. 25b and 29b). The rest of the behavioral patterns and the reasons behind are similar to the same configuration at pedestrian level. Some of these behavioral patterns include higher V_R values if compared to the random configuration at mid-level (Figs. 29a and 29b), decrease in V_R values as GBCR increases and the gradient of V_R decrease with GBCR increase gets steeper when lesser canyons are parallel to the wind orientation (i.e. 0˚ and 22.5˚ north).

3) Slab Blocks, Mid-Level - Courtyard Configuration:

In GBCR courtyard configuration for slab blocks at mid-level, the V_R values are generally higher than those from pedestrian level for the stronger wind at upper levels (Figs. 25c and 29c). Some of the behavioral patterns at mid-level that were similar to the same configuration at pedestrian level include lower V_R readings than group configuration at the same level (Figs. 29b and 29c) and the higher the number of canyons towards the wind orientation, the higher are the V_R readings. The reasons behind these behaviors are the same as the same configuration at pedestrian level.

The following phenomenon discussed will be slightly different from that of pedestrian level. For 67.5˚ and 90˚ north wind orientation cases, there is a slight increase in V_R as GBCR increases. This is due to the higher number of canyons which promotes channeling effects to occur while having the same precinct border lined up with slab blocks (Figs. 30a and 30b). The smaller influence of the massive wall surfaces against the wind compared to 0˚ north orientation winds also play a part. As for 22.5˚ and 45˚ north wind orientation cases, this trend increase is not too obvious. The reason being that at mid-levels, the disturbance from higher turbulence causes the wind to be further slowed down compared to that of pedestrian level where wind flow patterns are more stable to produce a slight increasing trend. Next, for the 0˚ north wind orientation cases, we can even see a slight decrease in V_R with GBCR increase. The possible explanation is that at mid-level, winds are relatively more turbulent compared to pedestrian level. Furthermore, due to the massive vertical wall surfaces facing the wind, 0˚ north wind orientation cases are the most affected. This increases the turbulence even more and causes the slight decrease in V_R with GBCR increase (Figs. 30c and 30d).

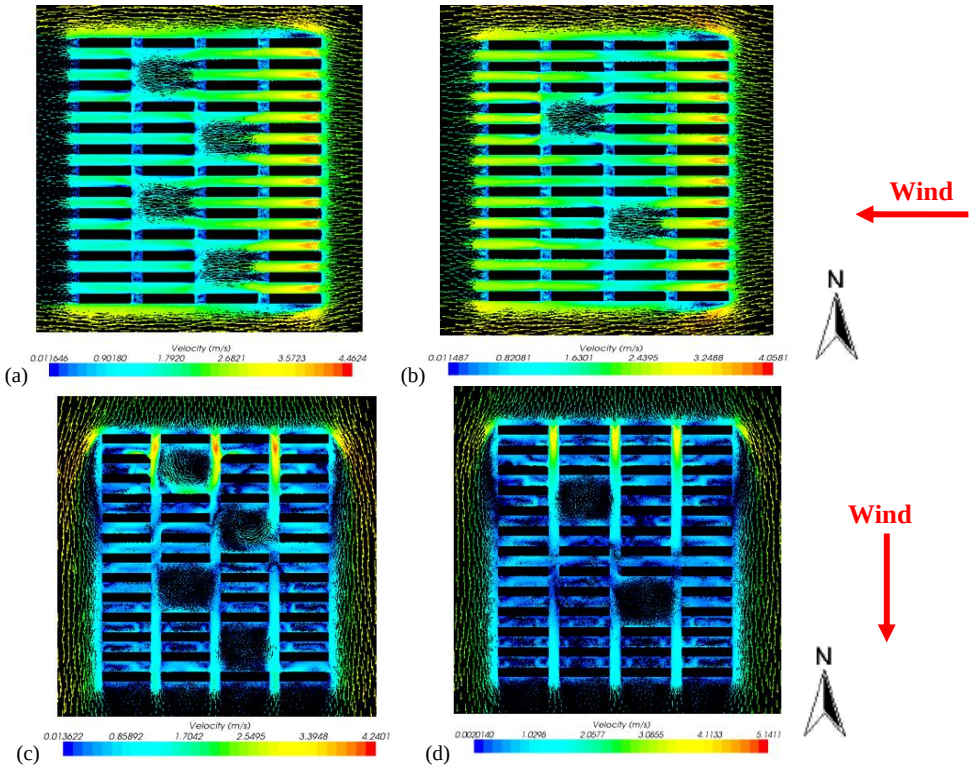

Fig. 30 Slab blocks, courtyard configuration:

(a) Velocity vectors for GBCR = 0.352 for wind from 90˚ north (mid-level)
(b) Velocity vectors for GBCR = 0.384 for wind from 90˚ north (mid-level)
(c) Velocity vectors for GBCR = 0.352 for wind from 0˚ north (mid-level)
(d) Velocity vectors for GBCR = 0.384 for wind from 0˚ north (mid-level)

V. CONCLUSIONS

The detailed parametric study on GBCR within a precinct area, carried out by the use of numerical simulation, shows that by using the same index proposed by Golany [9], it yields different consistent trends under the variation of different configurations, wind orientations and building types. The following are some of the main findings from the parametric study exercise.

For the point blocks, the following findings and explanations apply to both the pedestrian and mid-levels but with the mid-level readings being generally higher due to the stronger wind flow at upper levels. It is observed that for random configurations, most of the results show that with increasing GBCR, V_R decreases up to a certain value and then increases again. This phenomena show that the increase in roughness happens with increasing building numbers up to a certain point whereby further GBCR increase will start to create more urban canyons for channeling effects to take place. This applies to all the wind orientations except 45˚ north whereby it follows a reverse natural logarithmic curve (decreasing V_R curve with decreasing gradient) with GBCR increase. The reason for this is the higher degree of opposing wind flows from both transverse main canyon directions; hence GBCR exerts a greater effect than the channeling effects as mentioned for other wind orientation cases. For group configurations, the fully empty spaces and concentration of canyons tends to give higher V_R readings than random configurations. Furthermore, it follows the general findings from most researchers that a decrease in V_R occurs from low to high GBCR, as it is a straight forward consideration of building footprint coverage unlike the random configuration. For the courtyard configuration, V_R results are slightly lower than those of the group configuration. The buildings which bordered around the precinct act as blockages which prevented the wind from entering into the precinct. On the other hand, the V_R readings are comparable to those of the random configuration. The empty lumps of space may be the positive factor, whereas for random configuration, the non-enclosed border is a positive factor that offset the negativities of broken up empty spaces. Finally, the general increase of V_R with GBCR increase is due to the increase in effective canyons formed while having the precinct border lined up with buildings.

For the slab blocks, the following findings and explanations apply to both the pedestrian and mid-levels but with the mid-level readings being generally higher due to the stronger wind flow at upper levels. It is observed that in random configurations, the results show that the V_R for wind orientations like 0˚ and 22.5˚ north tends to decrease as GBCR increases; whereas for wind direction like 67.5˚ and 90˚ north, it follows a hump shape whereby as GBCR increases, V_R decreases up to a point and then starts to increase again. The number of canyons that are parallel to the wind direction is an important factor. The lesser the canyons that are parallel to the wind direction, the more V_R will be affected by GBCR coverage. On the other hand, the higher the number of canyons that are parallel to the wind, it gives rise to the increase in ground roughness with GBCR increase up to a threshold point. Further GBCR increase will lead to the formation of effective canyons that helps to advance the channeling effects of the whole precinct. For group configurations, the full empty spaces and concentration of canyons tends to generally give higher V_R readings than random configurations. Furthermore, when GBCR increases for all the wind orientations, a decrease in V_R occurs. The reason is similar to point blocks whereby the grouping of blocks plays an important role in increasing the surface roughness within a precinct as GBCR increases. But this decreasing trend of V_R with GBCR increase becomes less prominent when higher number of canyons are parallel to wind direction (e.g. for orientations like 67.5˚ and 90˚ north), indicating that GBCR influence decreases with the presence of more parallel canyons. For the courtyard configuration, V_R results are slightly lower than those of the group configuration. The buildings which bordered around the precinct act as blockages which prevented the wind from entering into the precinct. Next, the general increase of V_R with GBCR increase is due to the rise in effective canyons formed while having the precinct border lined up with buildings. The gradient of increasing trend increases when wind orientation changes from 0˚ to 90˚ north. This is due to the increase in channeling effects from the increase number of canyons and decreasing influence of the massiveness of wall surfaces against the wind. The same reasons are also the cause of the higher values of V_R for 67.5˚ north and 90˚ north orientated wind cases compared to the rest.

From the comprehensive simulation data, we can see that under different GBCR configurations (random, group and courtyard), consistent but different trends can be observed under the same GBCR value. This study sheds light on how buildings coverage and arrangements can affect outdoor ventilation within an estate or precinct and supports the initial hypothesis, on the correlation between building morphologies and the outdoor ventilation. These consistent patterns of behavior have important implications for building and urban planning development of residential estates in future and support the possibility of using GBCR index; together with other standardized morphological indices (which the author is currently working on e.g. Orientation, Geometry, Building Shape, etc.), as independent variables - to build an overall ventilation model using V_R as the dependent variable (a determinant of estate-level outdoor ventilation potential). One of this overall model's usefulness is to help facilitate the comparison of different proposed urban designs from planners during their initial design stage. Software packages like Geographical Information System (GIS) can be used to map out their different morphological indices, including GBCR, and input into this overall Wind Velocity Ratio Index (V_R) model. The results from the model will give a good indication of how the different indices, when combined, will affect or influence the ventilation potential of the whole estate. Problems of the urban design can be pinpointed during the early design stage before the construction begins, therefore helping to optimize good designs as early as possible. It is hoped that the data in this detailed simulation study of GBCR can be used for subsequent development of this overall ventilation model which will be useful for urban planning of high-rise precincts by building professionals.

NOMENCLATURE

ABL: Atmospheric boundary layer
α: Power-law exponent
BCA: Building and Construction Authority
BLWT: Boundary layer wind tunnel
CFD : Computational Fluid Dynamics
CUHK: Chinese University of Hong Kong
GBCR: Gross Building Coverage Ratio
GIS: Geographical Information System
HDB: Housing and Development Board
IRF: Isolated roughness flow
NEA: National Environment Agency
RANS: Reynolds-averaged Navier-Stokes
RLZ: Realizable k-ε turbulence model
Re: Reynolds number
SF: Skimming flow
UBL: Urban boundary layer
UCL: Urban canopy layer
VR: Wind Velocity Ratio
WIF: Wake interference flow
Z_0: Roughness length

REFERENCES

[1] M. Santamouris, *Energy and Climate in the Urban Built Environment*, UK: James and James (Science Publishers) Ltd, 2001.

[2] L. J. Hunter, G. T. Johnson, and I. D. Watson, "An investigation of three-dimensional characteristics of flow regimes within the urban canyon," *Atmospheric Environment*, vol. 26B, iss. 4, pp. 425-432, 1992.

[3] L. Adolphe, "A simplified model of urban morphology: application to an analysis of the environmental performance of cities," *Environment and Planning (B): Planning and Design*, vol. 28, iss. 2, pp. 183-200, 2001.

[4] J.-J. Kim and J.-J. Baik, "A numerical study of the effects of ambient wind direction on flow and dispersion in urban street canyons using the RNG k-ɛturbulence model," *Atmospheric Environment*, vol. 38, iss. 19, pp. 3039-3048, 2004.

[5] E. Ng, "Policies and technical guidelines for urban planning of high-density cities – air ventilation assessment (AVA) of Hong Kong," *Building and Environment*, vol. 44, pp. 1478-1488, 2009.

[6] J. A. Roberson and C. T. Crowe, *Engineering Fluid Mechanics*, USA: Wiley, 1988.

[7] G. Z. Brown and M. Dekay, *Sun, Wind and Light: Architectural Design Strategies*, 2nd ed., New York: Wiley, 2001.

[8] B. Givoni, *Climate Considerations in Building and Urban Design*, USA: Wiley, 1998.

[9] G. S. Golany, "Urban design morphology and thermal performance," *Atmospheric Environment*, vol. 30, iss. 3, pp. 455-465, 1996.

[10] T. Kubota, M. Miura, Y. Tominaga, and A. Mochida, "Wind tunnel tests on the relationship between building density and pedestrian-level wind velocity: Development of guidelines for realizing acceptable wind environment in residential neighborhoods," *Building and Environment*, vol. 43, iss. 10, pp. 1699-1708, 2008.

[11] T. R. Oke, "Street design and urban canopy layer climate," *Energy and Buildings*, vol. 11, iss. 1-3, pp. 103-113, 1988.

[12] A. Zhang, C-L. Gao, and L. Zhang, "Numerical simulation of the wind field around different building arrangements," *Journal of Wind Engineering and Industrial Aerodynamics*, vol. 93, pp. 891-904, 2005.

[13] L. J. Hunter, I. D. Watson, and G. T. Johnson, "Modeling air flow regimes in urban canyons," *Energy and Buildings*, vol. 15-16, iss. 3-4, pp. 315-324, 1990/1991.

[14] M. Hussain and B. E. Lee, "An Investigation of Wind Forces on Three-dimensional Roughness Elements in a Simulated Atmospheric Boundary Layer Flow – Part II. Flow Over Large Arrays of Identical Roughness Elements and the Effect of Frontal and Side Aspect Ratio Variations," Report No BS 56, Department of Building Sciences, University of Sheffield, 1980.

[15] J. F. Sini, S. Anquetin, and P. G. Mestayer, "Pollutant dispersion and thermal effects in urban street canyons," *Atmospheric Environment*, vol. 30, iss. 15, pp. 2659-2677, 1996.

[16] A. T. Chan, E. S. P. So, and S. C. Samad, "Strategic guidelines for street canyon geometry to achieve sustainable street air quality," *Atmospheric Environment*, vol. 35, iss. 32, pp. 5681-5691, 2001.

[17] X. Xie, Z. Huang, and J. S. Wang, "Impact of building configuration on air quality in street canyon," *Atmospheric Environment*, vol. 36, pp. 3601-3613, 2005c.

[18] R. W. MacDonald, R. F. Griffiths, and D. J. Hall, "An improved method for the estimation of surface roughness of obstacle arrays," *Atmospheric Environment*, vol. 32, iss. 11, pp. 1857-1864, 1998.

[19] M. R. Raupach, "Drag and drag partition on rough surfaces," *Boundary-layer Meteorology*, vol. 60, iss. 4, pp. 375-395, 1992.

[20] Ministry of National Development (MND), *Planning for Growth, Investing in our Future (URA Corporate Plan Seminar – 9 Feb 2007)*, Singapore: MND, 2007.

[21] A. K. Wong and S. H. K. Yeh, *Housing a nation – 25 years of public housing in Singapore*, Singapore: Housing and Development Board (HDB), 1985.

[22] Housing and Development Board (HDB), *Building Group, Public housing design guide: principles and practice*, Singapore: Housing and Development Board, 2005.

[23] H. Khoo and V. Su, "Scaling New Heights," *Urban Redevelopment Authority (URA) - Skyline (A bi-monthly Newsletter)*, pp. 6-8, Mar/April, 2007.

[24] Building and Construction Authority (BCA), *Building Planning and massing (Green Building Platinum Series)*, Singapore: BCA, 2010.

[25] T. -H. Shih, W. W. Liou, A. Shabbir, Z. Yang, and J. Zhu, "A new *k-ε* eddy viscosity model for high Reynolds number turbulent flows," *Computer Fluids*, vol. 24, iss. 3, pp. 227-238, 1995.

[26] T. L. Chan, G. Dong, C. W. Leung, C. S. Cheung, and W. T. Hung, "Validation of a two-dimensional pollutant dispersion model in an isolated street canyon," *Atmospheric Environment*, vol. 36, iss. 5, pp. 861-872, 2002.

[27] H. W. Han, "A study of entrainment in 2-phase upward concurrent annular flow in a vertical tube," PhD Thesis, University of Saskatchewan, 2005.

[28] C. Teodosiu and G. Rusaouen, "Modelisation des corps de chauffe a l'aide des codes de champ," *Proceedings of the Fourth Fluent Users Meetings – France*, Paris, France, 2000.

[29] J. C. DeBlois, M. M. Bilec, and L. A. Schaefer, "Design and zonal building energy modeling of a roof integrated solar chimney," *Renewable Energy*, vol. 52, pp. 241-250, 2013.

[30] B. Mohammadi, "Etude du modele *k-ε* de la turbulence pour les ecoulements compressibles," PhD thesis, Universite Paris VI, 1991.

[31] W. Xu, Q. Chen and F. T. M. Nieuwstadt, "A new turbulence model for near-wall natural convection," *International Journal of Heat and Mass Transfer*, vol. 41, iss. 21, pp. 3161-3176, 1998.

[32] R. X. Lee, S. K. Jusuf, and N. H. Wong, "The study of height variation on outdoor ventilation for Singapore's high-rise residential housing estates," *International Journal of Low-Carbon Technologies*, vol. 0, pp. 1-19, 2013.

[33] Building and Construction Authority (BCA), *Code for Environmental Sustainability of Buildings*, 3rd ed., Singapore: BCA, 2012.

[34] COST (Best Practice Guidelines for the CFD Simulation of Flows in the Urban Environment) - COST Action 732 (Quality Assurance and improvement of microscale meteorological models), University of Hamburg, Meteorological Institute, Centre for Marine and Atmospheric Sciences, Hamburg, Germany, 2007.

[35] B. C. Cochran, "The Influence of Atmospheric Turbulence on the Kinetic Energy Available During Small Wind Turbine Power Performance Testing," *IEA Expert Meeting on: Power Performance of Small Wind Turbines Not Connected to the Grid*, CEDER-CIEMAT, Soria, Spain, 2002.

[36] J. Wieringa, "Updating the Davenport roughness classification," *Journal of Wind Engineering and Industrial Aerodynamics*, vol. 41, iss. 1-3, pp. 357-368, 1992.

[37] F. T. De Paul and C. M. Shieh, "Measurements of Wind Velocities in a Street Canyon," *Atmospheric Environment*, vol. 20, iss. 3, pp. 455-459, 1986.

[38] R. Priyadarsini, K. W. Cheong, and N. H. Wong, "Enhancement of natural ventilation in high-rise residential buildings using stack system," *Energy and Buildings*, vol. 36, pp. 61-71, 2004.

[39] W. H. Rae and A. Pope, *Low-speed wind tunnel testing*, 2nd ed., USA: John Wiley and Sons, 1984.

[40] American Society of Civil Engineers (ASCE), *Wind Tunnel Studies of Buildings and Structures (ASCE Manuals and Reports on Engineering Practice No. 67)*, USA: ASCE, 1999.

[41] R. A. Bradley, "Wind-Tunnel Study of Cross Vault Structures," Master's Thesis, University of the Witwatersrand, Johannesburg, 2011.

[42] H. Liu, *Wind Engineering (A Handbook for Structural Engineers)*, University of Missouri-Columbia, Prentice Hall, Englewood Cliffs, New Jersey, 1990.

[43] CUHK, *Urban Climatic Map and Standards for Wind Environment – Feasibility Study Working Paper 1A: Draft Urban Climatic Analysis Map*, 2008.